Study of Electrical Conductivity of Epoxy/Graphene Platelet Nanocomposites

Shuaibo Yu

A thesis submitted to the

Faculty of Graduate and Postdoctoral Studies

in partial fulfillment of the requirements for the degree of

Master of Applied Science

in Chemical Engineering

Department of Chemical and Biological Engineering

Faculty of Engineering

University of Ottawa

May 2014

Abstract

Polymer nanocomposites are prepared by appropriately dispersing nanoscale fillers into polymer matrices. Graphene, a two-dimensional nano-carbon material with outstanding physical properties, has been widely studied as a conductive filler for nanocomposites. In this work, a gum Arabic aqueous solution was proposed as a new media to exfoliate graphite into few-layer graphene by liquid-phase sonication. Successful exfoliation was confirmed by Raman spectroscopy, scanning electron microscopy and transmission electron microscopy. Four types of graphene nanoplatelets were used to study the effects of the filler's aspect ratio. The one with the largest aspect ratio showed the best performance, where the conductivity of neat epoxy was increased by five orders of magnitude at 10 wt.%. Using a hot sonication technique and adding a small amount of second fillers further improved the electrical conductivities. The highest conductivity obtained in this study was 0.025 S/cm, which met the requirements of electromagnetic shielding material.

Résumé

Des nanocomposés polymériques furent préparés en dispersant des composés appropriés dans une matrice polymérique. L'utilisation du graphène, un matériel à deux dimensions à base de nano-carbone ayant des propriétés physiques remarquables, comme charge conductive lors de la production de tels nanocomposés est d'un intérêt considérable. Lors de ces études, une solution aqueuse de gomme arabique fut proposée pour exfolier du graphite en graphène par sonication en phase liquide. L'exfoliation fut confirmée par spectroscopie Raman, par microscopie électronique à balayage et par microscopie électronique à transmission. Quatre types de nano-plaquettes de graphène furent utilisés afin d'étudier l'effect de la charge de composé dans la matrice. Les nano-plaquettes avec le plus grand rapport de chargement, correspondant à 10% par masse, démontrèrent la meilleure performance, et la conductivité de l'époxy augmenta de cinq ordres de grandeur. La conductivité électrique fut davantage améliorée en utilisant une technique de sonication à haute température, et en chargeant de petites quantités d'un deuxième composé. La conductivité la plus élevée obtenue dans les matériels satisfaisant les exigences des matériaux de blindage électromagnétique, fut de 0.025 S/cm

Acknowledgment

Firstly, I would like to sincerely acknowledge my supervisor, Dr. Jason Zhang, for providing me the opportunity to pursue my Master's degree. His continuous guidance and support have been extensively helpful.

Secondly, I would like to thank my co-supervisor, Dr. Aiping Yu from the University of Waterloo, for her valuable guidance and beneficial discussions throughout this project. Her expertise in polymer nanocomposites was extremely helpful to my project.

Thirdly, I am grateful to all the colleagues in the lab at the University of Waterloo, for their selfless help on my research and experiments, especially, Victor Chabot, Kun Feng and Ariful Hoque.

Finally, I would like to thank my friends and family for their encouragement and support.

Table of Contents

List of Figures

List of Tables

Nomenclature

CB	Carbon black
CNF	Carbon nanofiber
CNT	Carbon nanotube
CVD	Chemical vapor deposition
EMI	Electromagnetic interference
FLG	Few-layer graphene
GA	Gum Arabic
GIC	Graphite intercalated compound
GO	Graphite oxide
LEG	Liquid-phase exfoliated graphene
NMP	N-methyl-pyrrolidone
SLG	Single-layer graphene
SEM	Scanning electron microscopy
TEM	Transmission electron microscopy
TGA	Thermogravimetric analysis
xGnP	Graphene nanoplatelet

CHAPTER 1：Introduction

Polymeric materials are extensively used in people's daily lives as well as in various industrial fields. In some cases, the properties of neat polymers are not quite sufficient for certain high demand applications. Appropriately adding high-quality fillers into a polymer matrix can significantly improve its performance or even endow some new properties to the polymer. When the filler has at least one dimension less than 100 nm, the resultant multi-phase material is known as a polymer nanocomposite. The first outstanding enhancement was demonstrated by the Toyota Motor Corporation in 1993, where the mechanical property of Nylon-6 was significantly enhanced by dispersing nano-clay in the matrix [1]. From then on, clay/polymer nanocomposites have been widely studied, based on almost every engineering polymer [2]. Since the discovery of graphene in 2004 [3], many researchers have moved their interests to studying this more amazing material as filler for polymer nanocomposites. The most dramatic change that graphene can bring to the polymer is the transition from electrically insulated to conductive. Electrical conductive polymer nanocomposites can be used for electromagnetic interference shielding as an alternative to metal based materials.

In order to fully exploit the potential of graphene/polymer nanocomposites, it is necessary to develop a way to produce high quality graphene in large quantities. It has been reported by many research groups that graphene can be produced by the direct exfoliation of graphite in an appropriate liquid medium [4-6]. In this study gum Arabic aqueous solution was selected as the new medium for the exfoliation of graphite.

It is known that the electrical conductivity of graphene/polymer nanocomposites strongly depends on the nature of the filler as well as the processing method [7]. Several key issues including the filler's aspect ratio, the dispersion state and the combination with a second-filler are identified and discussed in this thesis.

This thesis contains five chapters. Chapter 1 briefly introduces the background and motivation of this project; Chapter 2 gives a comprehensive review of literature in the area of nanocomposites regarding the production of graphene, the fabrication of composites, the resultant properties and potential applications; Chapter 3 demonstrates a new method to produce graphene on a large scale, which aims to provide a suitable source of graphene for nanocomposite applications; Chapter 4 presents the fabrication of graphene nanoplatelet /epoxy nanocomposites and the investigation of electrical conductivity. Finally, conclusions and recommendations are given in Chapter 5.

References

[1] Y. Kojima, A. Usuki, M. Kawasumi, A. Okada, Y. Fukushima, T. Kurauchi, O. Kamigaito, Mechanical properties of nylon 6-clay hybrid, J. Mater. Res. 8 (1993) 1185-1189.

[2] F. Gao, Clay/polymer composites: The story, Materials Today. 7 (2004) 50-55.

[3] K.S. Novoselov, A.K. Geim, S.V. Morozov, D. Jiang, Y. Zhang, S.V. Dubonos, I.V. Grigorieva, A.A. Firsov, Electric Field Effect in Atomically Thin Carbon Films, Science. 306 (2004) 666-669.

[4] A. Ciesielski, P. Samorì, Graphene via sonication assisted liquid-phase exfoliation, Chem. Soc. Rev. 43 (2013) 381-398.

[5] A. O'Neill, U. Khan, P.N. Nirmalraj, J. Boland, J.N. Coleman, Graphene Dispersion and Exfoliation in Low Boiling Point Solvents, J. Phys. Chem. C. 115 (2011) 5422-5428.

[6] Y. Hernandez, V. Nicolosi, M. Lotya, F.M. Blighe, Z. Sun, S. De, I.T. McGovern, B. Holland, M. Byrne, Y.K. Gun'Ko, J.J. Boland, P. Niraj, G. Duesberg, S. Krishnamurthy, R. Goodhue, J. Hutchison, V. Scardaci, A.C. Ferrari, J.N. Coleman, High-yield production of graphene by liquid-phase exfoliation of graphite, Nature Nanotechnology. 3 (2008) 563-568.

[7] R.M. Mutiso, K.I. Winey, 7.17 - Electrical Conductivity of Polymer Nanocomposites, in: K. Matyjaszewski, M. Möller (Eds.), Polymer Science: A Comprehensive Reference, Elsevier, Amsterdam, 2012, pp. 327-344.

CHAPTER 2：Literature Review

2.1 Introduction

Nano-scale fillers such as clays, silver nanoparticles，carbon black and carbon nanotubes (CNT) have been successfully dispersed in various polymers to produce polymer nanocomposites [1-4]. Compared to polymer composites with traditional micro-scale fillers such as carbon [5] or glass fiber [6]， nano-scale fillers can enhance the properties of neat polymers at much lower loadings. Graphene, a monolayer of carbon atoms arranged into a two-dimensional honeycomb lattice, was first isolated by two Russian scientists using a simple scotch tape peeling method [7]. The exciting physical properties of graphene include high electron mobility at room temperature, about 10000 cm^2/Vs [7], high thermal conductivity, up to 5300 W/mK [8]， a large Young's modulus of 1 TPa, [9] and good impermeability to standard gas (even the smallest gas atom) [10]. Graphene is harder than diamond, 300 times stronger than steel and conducts electricity much better than copper. These properties make graphene a great additive for improving the electrical, thermal, mechanical, and gas barrier properties of polymers. Benefiting from the rapid developments of efficient synthesis methods, graphene has become an excellent alternative to costly CNT as a multi-functional nano-filler for polymer composites [11].

This review will cover the recent advances in the area of graphene/polymer nanocomposites. To start, several synthesis methods of graphene are discussed and evaluated for composite applications. Then, commonly used techniques of preparing

graphene/polymer nanocomposites are reviewed. Finally, the properties of polymer composites with graphene dispersed inside, and their potential applications, are introduced.

2.2 Synthesis of Graphene

2.2.1 Micromechanical Exfoliation

Although graphene was first produced by growth on the surface of nickel in 1970 [12]， it was not considered stable alone until the successful isolation of single-layer graphene (SLG) in 2004, using micromechanical exfoliation [7]. This groundbreaking work allows the real properties of graphene to be measured, regardless of the effects of substrates.

Micromechanical exfoliation is a very simple scotch tape peeling method. The starting material, which is highly oriented pyrolytic graphite, was first prepared into 5 μm deep mesa by dry etching in oxygen plasma. The mesa was then attached to a photoresist layer and was ready to be peeled off by scotch tape. After repeated peeling, the thin flakes left in the photoresist layer were washed and transferred onto a silicon wafer. The presence of SLG was identified by atomic force microscopy (AFM). AFM images of SLG are shown in Figure 2-1. Although this method can produce high-quality and large-size SLG, it’s not suitable for polymer nanocomposite applications due to the low production rate.

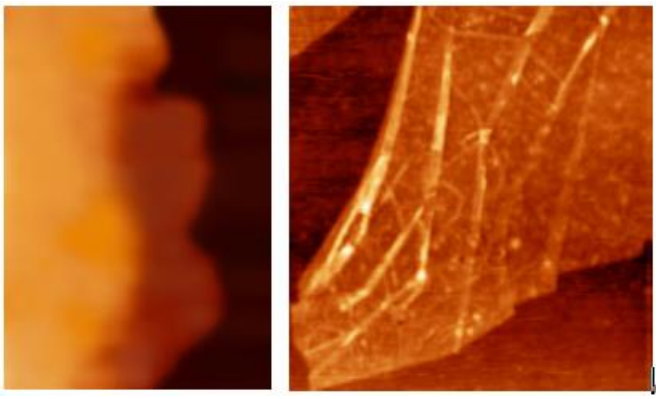

Figure 2-1 AFM images of SLG (left) and wrinkled SLG (Right)[7]

2.2.2 Chemical Vapor Deposition (CVD)

Chemical vapor deposition (CVD) on metal surfaces is another method used for the production of single-layer or few-layer graphene (FLG) films. The first successful synthesis of graphene by CVD was reported in 2006 using camphor as a precursor [13]. For a general CVD process, the Ni substrate is first exposed to a hydrocarbon gas mixture (H_2/CH_4) in a vacuum chamber below $1000°C$. In this step, hydrocarbon decomposes and dissolves into Ni substrate to form a solid solution. Graphene film is finally precipitated and formed on the Ni surface by cooling down the sample. The quality and the morphology of the graphene film can be controlled by the cooling rate and the microstructure of the Ni substrate respectively [14]. The ability of CVD to produce large area continuous graphene film makes it more attractive than the micromechanical exfoliation method for electronic applications [15], but still not a suitable source for polymer nanocomposite applications because of the low production rate and the high cost.

2.2.3 Exfoliation and Reduction of Graphite Oxide (GO)

The exfoliation and reduction of graphite oxide (GO) is a promising route for producing graphene on a large scale. GO is commonly prepared by Hummers method [16] and the improved method [17]. To be specific, graphite is oxidized by strong oxidants such as $KMnO_4$ and $NaNO_3$ in concentrated H_2SO_4 or a mixture of H_2SO_4/H_3PO_4. Similar to the relation between graphene and graphite, graphene oxide is s single-layer GO. There are two approaches to exfoliate GO into graphene oxide sheets and reduce it into graphene sheets.

The first approach is a chemical reduction. Typically, GO is dispersed and exfoliated in water by sonication and stirring to form a stable colloidal dispersion. The reducing agent (hydrazine hydrate) is then added into the solution. The reduced GO is obtained after 24 hours by heating the solution at $100°C$ [18]. Although the chemical reduction of graphene oxide is efficient, there are some drawbacks restricting its application, such as the toxicity and high cost of the reducing agent.

Thermal exfoliation and reduction of graphite oxide is another approach used to produce graphene sheets. Generally, GO is rapidly heated (>2000°C/min) to over 1000°C under inert gas [19]. The exfoliation and reduction are finished in one step which is an advantage of this thermal method. However the demand for high temperatures increases the cost of this method significantly.

Recently, several studies have been conducted to produce highly reduced GO with a high C/O ratio. Normally the C/O ratio is about 10/1 [20], but Dreyer and coworkers [21]

increased this number to 30/1 using benzyl alcohol (BnOH) as a reducing agent. In a patent invented in 2009 [22]， the ratio was further enlarged to 660/1 by an extended high temperature heat treatment (1500℃ for 2 min). Even so, complete reduction has not been achieved until now. Electrical conductivities are just partially restored from insulate GO. Compared to the high conductivity of pristine SLG (6000 S/cm) [23]， the reported value of reduced GO (46 S/cm) [21] is much lower. Although these routes can produce graphene on a large scale, they are not suitable sources for nanocomposite applications especially for electrically conductive polymers, due to the poor conductivity.

2.2.4 Liquid Phase Exfoliation of Graphite

Recently, graphite has been successfully exfoliated by sonication in liquid phase, in order to produce SLG or FLG. Unlike in the reduction of GO, the structure of pristine graphene is preserved, and fewer defects are introduced to the graphene sheet. The liquid media used for this method can be classified into three main categories: organic solvents, water/surfactant solutions and ionic liquids.

Hernandez et al.[24]demonstrated graphene dispersion with concentrations of up to 0.01mg/mL, with the dispersion and exfoliation of graphite in N-methyl-pyrrolidone (NMP). The yield of high-quality un-oxidized monolayer graphene sheets can be up to 12% of the starting graphite mass by recycling the sediments. In order to increase the yield, the same group demonstrated a method to prepare graphene dispersion in NMP by extended sonication, for up to 460 hours. Although the concentration was up to 1.2mg/mL, based on transmission electron microscopy (TEM), the size of the graphene sheets was reduced

after such a long period [25]. Other than NMP, several low boiling-point organic solvents such as chloroform, isopropanol and 1-propanol have also been investigated [26,27]. These solvents can easily be removed by air blowing.

Sodium cholate was used as a surfactant in Lotya's work [28]. The process used mild sonication for long periods (up to 400 hours), followed by controlled centrifugation to produce stable graphene dispersion. The highest concentration obtained was 0.3mg/mL. The sonication time was significantly shortened to 0.5 hours using another surfactant which is sodium dodecylbenzene sulphonate (SDBS). TEM results showed that more than 40% of flakes have less than five layers, and that the proportion of monolayer flakes was around 3% [29]. Zhang et al. took advantage of pyrene to produce high-quality single layer sheets and fabricate a super conductive transparent film (181200 S/m) [30]. The performances of a wide range of surfactants including ionic and non-ionic were compared by Guardia and coworkers [31]. As shown in Figure 2-2, after 2 hours of sonication with an initial graphite concentration of 100mg/mL, non-ionic surfactants generally perform better than ionic ones. The highest dispersion concentration can reach 0.9 mg/mL using P-123 (Pluronic®P-123).

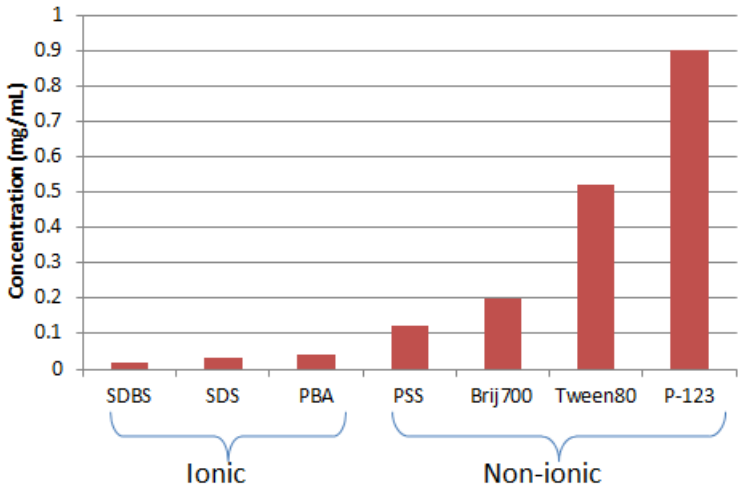

Figure 2-2 Concentration of graphene dispersions achieved by different surfactants， namely, sodium dodecyl sulphate (SDS), sodium dodecylbenzene-sulfonate (SDBS), 1-pyrenebutyric acid (PBA), poly(sodium 4-styrenesulfonate) (PSS), Brij700, Tween80 and Pluronic® P-123 (P-123).

Ionic liquid (IL) can be used as an alternative medium for the exfoliation of graphite, due to its similar surface energy [24] and the electrostatic interactions between IL and graphite [32]. Wang et al. [33] demonstrated direct exfoliation of graphite in 1-butyl-3-methylimidazolium bis(trifluoro-methane-sulfonyl) imide ([Bmim]-[Tf2N]) by tip sonication. High concentration (up to 0.95mg/mL) stable graphene dispersions were achieved after 60 minutes. By using another IL, 1-hexyl-3-methylimidazolium hexafluorophosphate (HMIH), a graphene dispersion with the highest ever reported concentration (5.33 mg/mL) was obtained.

Liquid phase exfoliation of graphite can produce high quality FLG or SLG and has the potential to be scaled up. The electrical conductivity reported was 20 times higher than that of reduced GO [34]. Mechanically strong graphene/polymer nanocomposites have been prepared by mixing this kind of graphene with poly (vinyl alcohol) [35] and polyurethane [36].

2.2.5 Intercalation of Small Molecules and Exfoliation

Right now, the most popular graphene production method for composite fillers is the intercalation of small molecules and exfoliation. The process starts from graphite intercalation compounds (GIC), also called expandable graphite. GIC is produced by the insertion of small molecules such as alkali metals [37] or acids [38,39] between graphite layers. The spacing between graphite layers is increased, and the interaction is impaired by intercalation [40]. GIC can be exfoliated by rapid heating [41], or by microwave treatment [42], to produce expanded graphite (EG). Graphene nanoplatelets (xGnP) with thicknesses in several nanometers were obtained by size reducing procedures, such as mechanical grinding or ultrasonication in organic solvents [43]. Although xGnP hasn't been fully exfoliated, and properties are compromised from that of single-layer graphene, it has the ability to improve the mechanical, thermal and electrical properties of nanocomposites [44,45] due to the pristine graphene structure and the high aspect ratio platelet shape. In addition, the cost of xGnP is only $5/lb which is much cheaper than other nano-scale carbon materials or than graphene produced by other methods. The production of xGnP is illustrated in Figure 2-3.

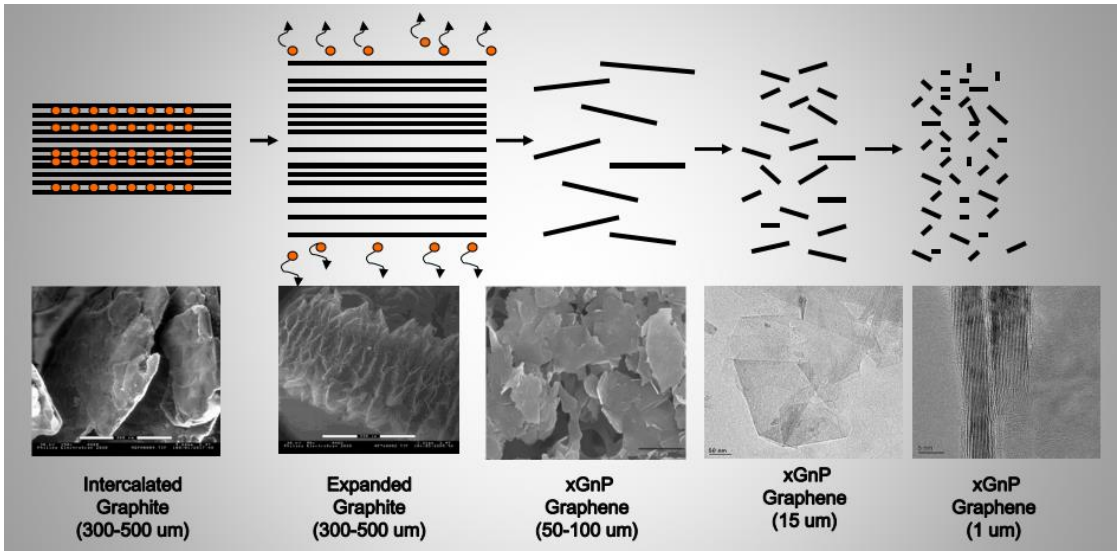

Figure 2-3 Illustration of the production of xGnP

2.3 Preparation Methods for Graphene/Polymer Nanocomposites

There are three main strategies to prepare graphene/polymer nanocomposites: solution blending, melt mixing and *in situ* polymerization.

2.3.1 Solution Blending

Solution blending is the simplest method of preparing graphene/polymer nanocomposites. For this technique, both graphene fillers and polymers are first dissolved in suitable solvents such as water or organic solvents by ultrasonication or by mechanical stirring. After the homogenous mixtures are obtained, the solvents can be removed by precipitation or simply by evaporation [40]. Composites based on water-soluble polymers such as poly(vinyl alcohol) (PVA) [46-49], poly(ethylene oxide) (PEO) [50], chitosan

[51], and poly(allylamine) [52] are normally produced by blending polymers with GO aqueous solutions, and then reducing the GO. Organic solvents such as acetone, dimethylformamide (DMF), chloroform and toluene have been used to dissolve a range of polymers including poly(methyl methacrylate) (PMMA) [47,53,54], polystyrene (PS) [55], polycarbonate [56], polyamides [57], polyethylene(PE) [58,59], polyurethane (PU) [60] and produce nanocomposites.

Since the dispersion of fillers strongly affects the properties of nanocomposites, several techniques such as the functionalization of graphene sheets, or stabilization by surfactants, have been employed to achieve good dispersion. For instance, GO was usually functionalized by isocyanate, nitrile and amine [61] or grafted by polymer [62]. Zhao et al. [46] used a 0.5 wt.% SDBS solution to disperse GO and produce graphene/PVA nanocomposites. Ultrasonication can be used to obtain metastable dispersion as well, however, defects in the graphene sheets might appear after a long exposure to powerful ultrasonication, and have a negative impact on composite properties [63]. Another issue with the solution blending method is the re-aggregation of graphene sheets during the slow solution removal step [3], evaporation times can be reduced by spin-casting [64] or drop-casting techniques [65].

2.3.2 Melt Mixing

Melt mixing is a scalable and economical method of preparing graphene/polymer nanocomposites. Graphene fillers are incorporated into polymer using high temperatures and shear force instead of solvents. Various polymers such as polypropylene

[66], poly (lacticacid) (PLA) [67,68], poly(vinylidenefluoride) (PVDF) [69] have been processed by this technique. A twin screw extruder is an essential piece of equipment for this process, as it can provide both high temperatures and shear force. Typically, polymer and dry graphene powders are manually mixed and are then fed into the extruder. In order to conduct mechanical or electrical testing, the wire-like samples are processed into thin films by compression moulding. Reduced GO is not a suitable filler for this method because of its instability to high temperatures and the polymers used for melt mixing are usually thermoplastic.

This processing technique is free from toxic and expensive solvents, however it still has several drawbacks, as follows: first and foremost, solvent mixing cannot provide the same dispersion level as the solution blending method [60,70]; secondly, the strong shear force may damage the graphene sheets and cause the reduction of the aspect ratio which can have negative effects on the composite properties [71]; finally, the miniscule and fluffy dry powder becomes a challenge when trying to feed it into the extruder [72]. To overcome these drawbacks, Steurer et al. [73] premixed the filler and polymer in acetone, and then dried the mixture and proceeded to the melt mixing. In another study, PP was coated with xGnP before the melt mixing, in order to get a more homogeneous mixture of filler and polymer [44]. Inversely, coating graphene with PP latex has also proved effective for improving the dispersion property [74], and a considerable improvement of the mechanical property was observed at a very low loading of graphene.

2.3.3 *In situ* Polymerization

Another commonly used fabrication technique for polymer nanocomposites is *in situ* polymerization. Plenty of polymers such as epoxy [75-79], PMMA [80-82], PE[83], and Nylon 6 [84,85] have been prepared with this technique. The general process involves the dispersion of a graphene-based filler with monomers followed by the polymerization or crosslinking reaction. A higher level of dispersion can be achieved with this method owing to the exfoliation of graphene layers by the insertion of monomers. In some systems [86-88], covalent linkages between functional groups of graphene sheets and polymer matrices were formed by a variety of chemical reactions. For instance, Fang et al. [87] functionalized graphene sheets with the initiator molecules of atom transfer radical polymerization (ATRP), then polystyrene chains were linked to graphene sheets during ATRP. 82 wt.% of PS chains were successfully grafted onto the surface of graphene sheets, resulting in good dispersion property and a controlled interface structure. Mechanical properties were considerably improved (70% for tensile strength, 57% for Young's modulus) using only a 0.9 wt.% of graphene sheets. Due to the high viscosity of monomer, solvents have to be employed for most cases， which causes the same concerns about solvent removal as in the solution blending method.

2.4 Properties and Applications of Graphene/Polymer Nanocomposites

Incorporating graphene into a polymer matrix with a proper fabrication technique can greatly improve the electrical, thermal, mechanical, and gas barrier properties of neat polymer. Theories and results of enhancements for the four properties above will be reviewed in this section, with an emphasis on the electrical properties. Various potential applications based on different properties will also be discussed.

2.4.1 Electrical Properties and Applications

The most notable property of graphene is its extraordinarily high electrical conductivity. The dispersion of graphene in a polymer matrix enables the transition of neat polymer from electrical insulator to electrical conductor. A conductive pathway can be formed within the polymer matrix when enough graphene is properly dispersed. This critical filler concentration is called the percolation threshold. A sharp increase in conductivity can be observed at the percolation threshold, and the conductivity of composites follow a power-law expression above the percolation threshold:

$$\sigma_c = \sigma_f(\phi - \phi_c)^t$$

Where σ_c is the conductivity of the composite (S/cm), σ_f is the conductivity of the filler (S/cm), ϕ is the volume concentration of the filler (vol%), ϕ_c is the percolation threshold (vol%) , and t is a scaling exponent [89].

Electrically conductive graphene/polymer nanocomposties have been successfully synthesized based on epoxy [90-92], polystyrene [55,93], polyurethane [60,94],

polycarbonate [95,96], polyester [96] and vinyl polymers[97,98]. Research objectives are either to reduce percolation thresholds or to increase electrical conductivities by modifying materials or processing techniques.

Stankovich et al.[55] reported the lowest percolation threshold for graphene based nanocomposites with only 0.1 vol%. Phenyl isocyanate-treated GO was dispersed in a polystyrene matrix, followed by a chemical reduction. The graphite was completely exfoliated and dispersed at the molecular level by solution blending. Thermally reduced GO (TRG) exhibits higher electrical conductivity than chemical reduced GO, due to the rareness of the oxygenated functional groups, and is more suitable for the melt mixing process because of its the thermal stability. Steurer et al. [73] produced a series of electrical conductive polymer nanocomposites with TRG by melt mixing. Percolation thresholds were found to be lower than zero-dimensional (carbon black) and one-dimensional (multi-wall nanotube) fillers. Yoonessi et al. reported a low percolation threshold at 0.14 vol% and high electrical conductivity of 51.2 S/m at 2.2 vol% for TRG/polycarbonate nanocomposites produced by positioning conductive graphene fillers on the surface polycarbonate microspheres [99]. The highest conductivity obtained so far was 1083.3 S/m at 4.8 vol% loading of graphene into a PS matrix resulting from the formation of a compact conductive network of graphene by a unique self-assembly process [100].

As mentioned before, xGnP derived from graphite intercalated compound has received a great deal of attention recently because of its high intrinsic electrical

conductivity, high aspect ratio, and cost effectiveness. Drzal and his group first proposed the production of xGnP in 2003 [42] and made massive efforts to use their products in nanocomposites applications. The first matrix material studied by them was epoxy [42]. In this initial work, xGnP treated by acrylamide grafting showed improved dispersion and adhesion in an epoxy matrix. The percolation threshold was observed at 1.93 wt.% and the conductivity of composites was 2.56 S/m at 7 wt.% loading. Results were superior to those obtained by vapor grown carbon fiber and by conventional carbon fiber. Afterwards, they comprehensively investigated various factors that could affect the percolation threshold and electrical conductivity, including the filler's geometry, intrinsic electrical conductivity, alignment and dispersion within the polymer, and the crystallinity of polymer based on the polypropylene matrix [101]. A low percolation threshold, 0.6 wt.% was obtained by a premixing method followed by compression moulding [44]. This newly developed method has proven effective for lowering the percolation threshold because of its ability to preserve the large platelet morphology of xGnP[102]. However, the percolation threshold can be very different for different polymer matrices. For instance, a much higher percolation threshold (12 wt.%) was found with linear low-density polyethylene (LLDPE) [103]. For xGnP/polyamide 6 (PA6) nanocomposites, the melt mixing method using the counter rotation twin screw provided a better dispersion of xGnP, therefore resulting in higher electrical conductivity than with the co-rotation twin screw extruder [104].

Using xGnP as an efficient filler for polymer nanocomposites has also been studied by other groups. Zaman et al. successfully lowered the percolation threshold of

xGnP/epoxy nanocomposites to 0.51wt.% by modifying the graphene sheet with polyoxyalkyleneamine [78]. Two different solvent-assisted methods for making xGnP/epoxy nanocomposites were compared by Monti and coworkers: the dispersion of monomer in xGnP/chloroform followed by the addition of hardener and the dispersion of hardener in xGnP/tetrahydrofuran followed by the addition of monomer. The first one showed a slightly better dispersion and a lower percolation threshold in comparison to the second one [91]. The three-roll mill appeared to be more effective than traditional sonication and high-speed shear mixing for the dispersion of xGnP into the epoxy matrix and showed a three orders higher electrical conductivity for the same loading [45]. Ma et al.[105] created a covalently bonded filler-matrix interface by using 4,4'-diaminodi-phenylsulfone (DDS) as a modifier to prevent the stacking of graphene sheets in the epoxy matrix. An eight-order improvement of electrical conductivity was obtained at 0.49 vol% for modified composites while no improvement was observed for the unmodified one.

Other than the modification of graphene sheets and variations in the processing methods, the filler's aspect ratio [106,107], sheet-sheet junctions [108], wrinkles and folds of graphene sheets [109] and particle alignments [110,111] have also been reported to affect the percolation threshold and conductivity. Notably, when the conductive network is formed in a polymer matrix, nanofillers do not necessarily make direct contact, and current flow can occur between thin polymer layers around nanofillers, which is known as the tunneling effect. The resistance derived from the tunneling effect is called

tunneling resistance, and it sometimes dominates over contact resistance which is considered as a limiting factor for composite conductivity [112,113].

The main applications of conductive polymer nanocomposites are based on electromagnetic interference (EMI) shielding, where the conductivity needs to be greater than 1 S/m [114]. It is important to absorb or reflect the electromagnetic waves emitted by electronic devices for the protection of other nearby devices, or even the health of human bodies. Compared to traditional metallic fillers, graphene can provide sufficient conductivity at much lower loadings due to its high intrinsic conductivity and aspect ratio [115]. As a result, EMI shielding materials based on graphene/polymer nanocomposites are light in weight and easy to be processed into any desired shape, which is particularly suitable for portable devices such as laptops and cell phones. Liang et al. successfully prepared lightweight and effective EMI shielding materials based on graphene/epoxy nanocomposites with a high shielding effectiveness of 21 db at 15 wt.% [90]. Conductive composites with relatively lower conductivities (10^{-4}~1 S/m) can be used for a similar application, electrostatic dissipation (ESD) [116]. Conductive graphene/polymer nanocomposites can also be applied to gas molecules [117,118], pH [119], pressure[120], temperature [97] sensors, Li-ion battery [121] or supercapacitor electrodes [122-124] and transparent electrodes for solar cells [125-127].

2.4.2 Thermal Properties and Applications

Graphene with excellent thermal conductivity has been used to make polymer nanocomposites with improved thermal conductivity or thermal stability. Unlike the

percolation theory for electrical conductivity, thermal energy is chiefly transferred via lattice vibration (phonons). The poor conduction at filler-matrix or filler-filler interfaces will hamper the increase of thermal conductivity for composites [128,129]. Additionally, the smaller difference (4 orders of magnitude) of thermal conductivities between graphene and neat polymer, compared to the huge difference (15-19 orders of magnitude) of electrical conductivities between the two also makes the enhancement of thermal properties not as significant as that of electrical properties [63]. However, other factors that could affect the electrical properties of nanocomposites such as shape and aspect ratio, dispersion and alignment of fillers are also applicable for thermal properties. For instance, it has been demonstrated that 2D platelet-like xGnPs are more effective than 1D rod-like carbon nanotubes or carbon nanofibers for thermal conductivity enhancement [130,131]. Thermal conductivity enhancements based on the epoxy matrix have been widely studied [41,132-134]. Yu et al. prepared xGnP with different aspect ratios with the intercalation of acid and controlled thermal expansion. The one with the largest aspect ratio (200) was most effective in enhancing thermal conductivity; a 30-fold increase from neat epoxy was obtained at 25 vol% loading [41]. In another study, graphene and multi-layer graphene were incorporated into epoxy and a 23-fold thermal conductivity enhancement at 10 vol% was achieved [135]. This exciting result was attributed to graphene's high aspect ratio and lower interface resistance. However, less significant improvements in thermal conductivities were observed for other matrices such as PP [136] and nylon [137]. Graphene/polymer nanocomposites with high thermal conductivities can

be used as a new class of thermal interface materials for thermal management in electronic devices [138].

Thermal stability can also be improved by embedding graphene into a polymer matrix. The degradation temperature of ionic liquid functionalized graphene/polystyrene composites was nearly 100℃ higher than that of pure polymer, which can be explained by the restriction of chain mobility by a strong filler-matrix interaction [93]. Similar phenomena have been found for other polymers such as PVA [139,140] and PMMA [141]. Graphene can be used as an alternative to flame-retardant additives to reduce the flammability of polymer, due to the formation of jammed network during combustion [142].

2.4.3 Mechanical Properties and Applications

As the strongest material ever measured, graphene has a Young's modulus of 1 TPa and an intrinsic strength of 130 GPa [9]. The addition of graphene into a polymer matrix can remarkably alter its mechanical property. King et al. [143] improved the tensile modulus of neat epoxy by 124% (from 2.72 GPa to 3.36 GPa) with 6 wt.% xGnP dispersed in the matrix. Rafiee and colleagues compared the efficiency of xGnP for mechanical property enhancements with SWNT and MWNT at low loadings. Graphene outperformed carbon nanotube fillers in terms of Young's modulus (28%), ultimate tensile strength (26%), and fracture toughness (33%). The high specific surface area, strong filler-matrix interaction, and unique platelet shape of graphene may lead these advantages [144]. Incorporating xGnP into a rubbery matrix can more distinctly improve

mechanical properties more pronouncedly due to the much lower modulus of the matrix. For instance, the tensile strength, Young's modulus, and tear strength of xGnP/ styrene butadiene rubber (SBR) nanocomposites were improved by 230%, 506% and 445% respectively [145]. However, for most cases, the ductilities of composites significantly decreased due to the addition of stiff filler [73].

Graphene/polymer nanocomposites with enhanced mechanical properties can be used as light structural components for aircrafts or automobiles [63,143].

2.4.4 Gas Barrier Properties and Applications

It has been reported that defect free graphene sheets are impermeable to all standard gases [10]. Incorporating two-dimensional graphene sheets with polymers provides more effective barrier properties than one-dimensional CNT and CNF or zero-dimensional carbon black. The formation of a percolation network alters the path of molecule diffusion, thus reducing the permeability of the polymer matrix. It has been suggested that a higher aspect ratio and a better alignment of graphene sheets can further enhance the barrier properties [146]. Such gas impermeable films can potentially be used for food packaging applications.

2.5 Concluding Remarks

Attracted by its exceptional physical properties, researchers from all over the world are now studying graphene. A variety of methods have been developed to produce high quality or large scale graphene. As a result of this rapid development, the price of graphene has significantly decreased, thus making a lot of applications possible, especially for polymer nanocomposites, which require a large amount of high quality but inexpensive graphene sheets. Micromechanical exfoliated and CVD grown graphene sheets possess very good qualities with a controlled number of layers and large sheet areas. However, manually peeling from graphite is very ineffective, and CVD growing methods also have very low production scale. Currently, the most widely studied graphene for nanocomposites is based on the exfoliation and reduction of GO, due to its large scale production, despite the fact that the quality is compromised compared to defect-free graphene sheets. The intercalation of small molecules and exfoliation is another popular method for the large scale production of graphene nanoplatelets. Thus-produced graphene nanoplatelets have been commercialized as low-cost multi-functional fillers for nanocomposites. Recently, graphene has been successfully synthesized via the liquid phase exfoliation. The non-oxidized process preserves the pristine structure of graphene sheets and has a great potential to be scaled up for nanocomposite applications.

Various routes have been developed to disperse graphene fillers into polymer matrices. Based on different types of polymers, nanocomposites can be prepared by

solution blending, melt mixing and *in-situ* polymerization. Numerous efforts have been devoted to the production of high performance graphene/polymer nanocomposites with relative lower loadings of graphene. Polymer nanocomposites are extremely versatile and can be used for many applications including electronics, aerospace, automotive, and packaging.

References

[1] A. Usuki, A. Koiwai, Y. Kojima, M. Kawasumi, A. Okada, T. Kurauchi, O. Kamigaito, Interaction of nylon 6-clay surface and mechanical properties of nylon 6-clay hybrid, J Appl Polym Sci. 55 (1995) 119-123.

[2] H. Tang, X. Chen, Y. Luo, Electrical and dynamic mechanical behavior of carbon black filled polymer composites, European Polymer Journal. 32 (1996) 963-966.

[3] M. Moniruzzaman, K.I. Winey, Polymer Nanocomposites Containing Carbon Nanotubes, Macromolecules. 39 (2006) 5194-5205.

[4] L. Vescovo, M. Sangermano, R. Scarazzini, G. Kortaberria, I. Mondragon, In-situ-Synthetized Silver/Epoxy Nanocomposites: Electrical Characterization by Means of Dielectric Spectroscopy, Macromol. Chem. Phys. 211 (2010) 1933-1939.

[5] Y. Chekanov, R. Ohnogi, S. Asai, M. Sumita, Electrical properties of epoxy resin filled with carbon fibers, J. Mater. Sci. 34 (1999) 5589-5592.

[6] W. Gu, H.F. Wu, S.L. Kampe, G.-. Lu, Volume fraction effects on interfacial adhesion strength of glass-fiber-reinforced polymer composites, Materials Science and Engineering: A. 277 (2000) 237-243.

[7] K.S. Novoselov, A.K. Geim, S.V. Morozov, D. Jiang, Y. Zhang, S.V. Dubonos, I.V. Grigorieva, A.A. Firsov, Electric Field Effect in Atomically Thin Carbon Films, Science. 306 (2004) 666-669.

[8] A.A. Balin, S. Ghosh, W. Bao, I. Calizo, D. Teweldebrhan, F. Miao, C.N. Lau, Superior Thermal Conductivity of Single-Layer Graphene, Nano Letters. 8 (2008) 902-907.

[9] C. Lee, X. Wei, J.W. Kysar, J. Hone, Measurement of the Elastic Properties and Intrinsic Strength of Monolayer Graphene, Science. 321 (2008) 385-388.

[10] J.S. Bunch, S.S. Verbridge, J.S. Alden, A.M.v.d. Ze, J.M. Parpia, H.G. Craighead, P.L. McEuen, Impermeable Atomic Membranes from Graphene Sheets, Nano Letters. 8 (2008) 2458-2462.

[11] L.T. Drzal, H. Fukushima, Exfoliated graphite nanoplatelets (xGnP): A carbon nanotube alternative, 2006 NSTI Nanotechnology Conference and Trade Show - NSTI Nanotech 2006 Technical Proceedings. 1 (2006) 170-173.

[12] J.M. Blakely, J.S. Kim, H.C. Potter, Segregation of Carbon to the (100) Surface of Nickel, J. Appl. Phys. 41 (1970) 2693-2697.

[13] P.R. Somani, S.P. Somani, M. Umeno, Planer nano-graphenes from camphor by CVD, Chemical Physics Letters. 430 (2006) 56-59.

[14] Y. Zhang, L. Zhang, C. Zhou, Review of Chemical Vapor Deposition of Graphene and Related Applications, Acc. Chem. Res. 46 (2013) 2329-2339.

[15] A. Reina, X. Jia, J. Ho, D. Nezich, H. Son, V. Bulovic, M.S. Dresselhaus, K. Jing, Large area, few-layer graphene films on arbitrary substrates by chemical vapor deposition, Nano Letters. 9 (2009) 30-35.

[16] W.S. Hummers Jr., R.E. Offeman, Preparation of graphitic oxide, J. Am. Chem. Soc. 80 (1958) 1339.

[17] D.C. Marcano, D.V. Kosynkin, J.M. Berlin, A. Sinitskii, Z. Sun, A. Slesarev, L.B. Alemany, W. Lu, J.M. Tour, Improved synthesis of graphene oxide, ACS Nano. 4 (2010) 4806-4814.

[18] S. Stankovich, D.A. Dikin, R.D. Piner, K.A. Kohlhaas, A. Kleinhammes, Y. Jia, Y. Wu, S.T. Nguyen, R.S. Ruoff, Synthesis of graphene-based nanosheets via chemical reduction of exfoliated graphite oxide, Carbon. 45 (2007) 1558-1565.

[19] H.C. Schniepp, J. Li, M.J. McAllister, H. Sai, M. Herrera-Alonso, D.H. Adamson, R.K. Prud'homme, R. Car, D.A. Saville, I.A. Aksay, Functionalized Single Graphene Sheets Derived from Splitting Graphite Oxide, The Journal of Physical Chemistry B. 110 (2006) 8535-8539.

[20] M.J. McAllister, J.-. Li, D.H. Adamson, H.C. Schniepp, A.A. Abdala, J. Liu, M. Herrera-Alonso, D.L. Milius, R. Car, R.K. Prud'homme, I.A. Aksay, Single sheet functionalized graphene by oxidation and thermal expansion of graphite, Chemistry of Materials. 19 (2007) 4396-4404.

[21] D.R. Dreyer, S. Murali, Y. Zhu, R.S. Ruoff, C.W. Bielawski, Reduction of graphite oxide using alcohols, Journal of Materials Chemistry. 21 (2011) 3443-3447.

[22] I.A. - Aksay, D.L. - Milius, S. - Korkut, R.K. - Prud'homme, - Functionalized graphene sheets having high carbon to oxygen ratios, US Patent, (2010) EP20090739294 .

[23] X. Du, I. Skachko, A. Barker, E.Y. Andrei, Approaching ballistic transport in suspended graphene, Nature Nanotechnology. 3 (2008) 491-495.

[24] Y. Hernandez, V. Nicolosi, M. Lotya, F.M. Blighe, Z. Sun, S. De, I.T. McGovern, B. Holland, M. Byrne, Y.K. Gun'Ko, J.J. Boland, P. Niraj, G. Duesberg, S. Krishnamurthy, R. Goodhue, J. Hutchison, V. Scardaci, A.C. Ferrari, J.N. Coleman, High-yield production of graphene by liquid-phase exfoliation of graphite, Nature Nanotechnology. 3 (2008) 563-568.

[25] U. Khan, A. O'Neill, M. Lotya, S. De, J.N. Coleman, High-Concentration Solvent Exfoliation of Graphene, Small. 6 (2010) 864-871.

[26] A. O'Neill, U. Khan, P.N. Nirmalraj, J. Boland, J.N. Coleman, Graphene Dispersion and Exfoliation in Low Boiling Point Solvents, J. Phys. Chem. C. 115 (2011) 5422-5428.

[27] E. Choi, W.S. Choi, Y.B. Lee, Y. Noh, Production of graphene by exfoliation of graphite in a volatile organic solvent, Nanotechnology. 22 (2011) 365601.

[28] M. Lotya, P.J. King, U. Khan, S. De, J.N. Coleman, High-Concentration, Surfactant-Stabilized Graphene Dispersions, ACS Nano. 4 (2010) 3155-3162.

[29] M. Lotya, Y. Hernandez, P.J. King, R.J. Smith, V. Nicolosi, L.S. Karlsson, F.M. Blighe, S. De, Z. Wang, I.T. McGovern, G.S. Duesberg, J.N. Coleman, Liquid Phase Production of Graphene by Exfoliation of Graphite in Surfactant/Water Solutions, J. Am. Chem. Soc. 131 (2009) 3611-3620.

[30] M. Zhang, R.R. Parajuli, D. Mastrogiovanni, B. Dai, P. Lo, W. Cheung, R. Brukh, P.L. Chiu, T. Zhou, Z. Liu, E. Garfunkel, H. He, Production of Graphene Sheets by Direct Dispersion with Aromatic Healing Agents, Small. 6 (2010) 1100-1107.

[31] L. Guardia, M.J. Fernández-Merino, J.I. Paredes, P. Solís-Fernández, S. Villar-Rodil, A. Martínez-Alonso, J.M.D. Tascón, High-throughput production of pristine graphene in an aqueous dispersion assisted by non-ionic surfactants, Carbon. 49 (2011) 1653-1662.

[32] W. Du, X. Jiang, L. Zhu, W. Du, X. Jiang, L. Zhu, From graphite to graphene: direct liquid-phase exfoliation of graphite to produce single- and few-layered pristine graphene, Journal of Materials Chemistry A. 1 (2013) 10592-10606.

[33] X. Wang, P.F. Fulvio, G.A. Baker, G.M. Veith, R.R. Unocic, S.M. Mahurin, M. Chi, S. Dai, Direct exfoliation of natural graphite into micrometre size few layers graphene sheets using ionic liquids, Chem. Commun. 46 (2010) 4487-4489.

[34] V. Chabot, B. Kim, B. Sloper, C. Tzoganakis, A. Yu, High yield production and purification of few layer graphene by Gum Arabic assisted physical sonication, Science Reports. 3 (2013).

[35] P. May, U. Khan, A. O'Neill, J.N. Coleman, Approaching the theoretical limit for reinforcing polymers with graphene, Journal of Materials Chemistry. 22 (2012) 1278-1282.

[36] U. Khan, P. May, A. O'Neill, J.N. Coleman, Development of stiff, strong, yet tough composites by the addition of solvent exfoliated graphene to polyurethane, Carbon. 48 (2010) 4035-4041.

[37] L.M. Viculis, J.J. Mack, O.M. Mayer, H.T. Hahn, R.B. Kaner, Intercalation and exfoliation routes to graphite nanoplatelets, J. Mater. Chem. 15 (2005) 974-978.

[38] K.E. Carr, Intercalation and oxidation effects on graphite of a mixture of sulphuric and nitric acids, Carbon. 8 (1970) 155-166.

[39] G. Chen, D. Wu, W. Weng, C. Wu, Exfoliation of graphite flake and its nanocomposites, Carbon. 41 (2003) 619-621.

[40] J.R. Potts, D.R. Dreyer, C.W. Bielawski, R.S. Ruoff, Graphene-based polymer nanocomposites, Polymer. 52 (2011) 5-25.

[41] A. Yu, P. Ramesh, M.E. Itkis, E. Bekyarova, R.C. Haddon, Graphite Nanoplatelet-Epoxy Composite Thermal Interface Materials, Journal of Physical Chemistry C. 111 (2007) 7565-7569.

[42] H. Fukushima, Graphite nanoreinforcements in polymer nanocomposites, ProQuest Dissertations and Theses. (2003).

[43] B.Z. Jang, A. Zhamu, Processing of nanographene platelets (NGPs) and NGP nanocomposites: A review, J. Mater. Sci. 43 (2008) 5092-5101.

[44] H.-. Park, K. Kalaitzidou, H. Fukushima, L.T. Drzal, Exfoliated graphite nanoplatelet (xGnP)/polypropylene nanocomposites, SPE Automotive and Composites Divisions - 7th Annual Automotive Composites Conference and Exhibition, ACCE 2007 - Driving Performance and Productivity. 1 (2007) 314-322.

[45] S. Chandrasekaran, C. Seidel, K. Schulte, Preparation and characterization of graphite nano-platelet (GNP)/epoxy nano-composite: Mechanical, electrical and thermal properties, European Polymer Journal. 49 (2013) 3878-3888.

[46] X. Zhao, Q. Zhang, D. Chen, P. Lu, Enhanced Mechanical Properties of Graphene-Based Poly(vinyl alcohol) Composites, Macromolecules. 43 (2010) 2357-2363.

[47] B. Das, K. Eswar Prasad, U. Ramamurty, C.N.R. Rao, Nano-indentation studies on polymer matrix composites reinforced by few-layer graphene, Nanotechnology. 20 (2009) 1-5.

[48] L. Jiang, X.-. Shen, J.-. Wu, K.-. Shen, Preparation and characterization of graphene/poly(vinyl alcohol) nanocomposites, J Appl Polym Sci. 118 (2010) 275-279.

[49] R.K. Layek, S. Samanta, A.K. Nandi, The physical properties of sulfonated graphene/poly(vinyl alcohol) composites, Carbon. 50 (2012) 815-827.

[50] Y. Matsuo, K. Tahara, Y. Sugie, Structure and thermal properties of poly(ethylene oxide)-intercalated graphite oxide, Carbon. 35 (1997) 113-120.

[51] X. Yang, Y. Tu, L. Li, S. Shang, X. Tao, Well-Dispersed Chitosan/Graphene Oxide Nanocomposites, ACS Appl. Mater. Interfaces. 2 (2010) 1707-1713.

[52] A. Satti, P. Larpent, Y. Gun'Ko, Improvement of mechanical properties of graphene oxide/poly(allylamine) composites by chemical crosslinking, Carbon. 48 (2010) 3376-3381.

[53] T. Ramanathan, A.A. Abdala, S. Stankovich, D.A. Dikin, M. Herrera-Alonso, R.D. Piner, D.H. Adamson, H.C. Schniepp, X. Chen, R.S. Ruoff, S.T. Nguyen, I.A. Aksay, R.K. Prud'Homme, L.C. Brinson, Functionalized graphene sheets for polymer nanocomposites, Nature Nanotechnology. 3 (2008) 327-331.

[54] H. Zhang, W. Zheng, Q. Yan, Z. Jiang, Z. Yu, The effect of surface chemistry of graphene on rheological and electrical properties of polymethylmethacrylate composites, Carbon. 50 (2012) 5117-5125.

[55] S. Stankovich, D.A. Dikin, G.H.B. Dommett, K.M. Kohlhaas, E.J. Zimney, E.A. Stach, R.D. Piner, S.T. Nguyen, R.S. Ruoff, Graphene-based composite materials, Nature. 442 (2006) 282-286.

[56] A.L. Higginbotham, J.R. Lomeda, A.B. Morgan, J.M. Tour, Graphite oxide flame-retardant polymer nanocomposites, ACS Applied Materials and Interfaces. 1 (2009) 2256-2261.

[57] D. Chen, H. Zhu, T. Liu, In situ thermal preparation of polyimide nanocomposite films containing functionalized graphene sheets, ACS Applied Materials and Interfaces. 2 (2010) 3702-3708.

[58] H. Kim, S. Kobayashi, M.A. AbdurRahim, M.J. Zhang, A. Khusainova, M.A. Hillmyer, A.A. Abdala, C.W. Macosko, Graphene/polyethylene nanocomposites: Effect of polyethylene functionalization and blending methods, Polymer. 52 (2011) 1837-1846.

[59] Y. Chen, Y. Qi, Z. Tai, X. Yan, F. Zhu, Q. Xue, Preparation, mechanical properties and biocompatibility of graphene oxide/ultrahigh molecular weight polyethylene composites, European Polymer Journal. 48 (2012) 1026-1033.

[60] H. Kim, Y. Miura, C.W. MacOsko, Graphene/polyurethane nanocomposites for improved gas barrier and electrical conductivity, Chemistry of Materials. 22 (2010) 3441-3450.

[61] P.-. Ren, D.-. Yan, T. Chen, B.-. Zeng, Z.-. Li, Improved properties of highly oriented graphene/polymer nanocomposites, J Appl Polym Sci. 121 (2011) 3167-3174.

[62] G. Gonalves, P.A.A.P. Marques, A. Barros-Timmons, I. Bdkin, M.K. Singh, N. Emami, J. Grácio, Graphene oxide modified with PMMA via ATRP as a reinforcement filler, Journal of Materials Chemistry. 20 (2010) 9927-9934.

[63] V. Singh, D. Joung, L. Zhai, S. Das, S.I. Khondaker, S. Seal, Graphene based materials: Past, present and future, Progress in Materials Science. 56 (2011) 1178-1271.

[64] M.L. de la Chapelle, C. Stéphan, T.P. Nguyen, S. Lefrant, C. Journet, P. Bernier, E. Munoz, A. Benito, W.K. Maser, M.T. Martinez, G.F. de la Fuente, T. Guillard, G. Flamant, L. Alvarez, D. Laplaze, Raman characterization of singlewalled carbon nanotubes and PMMA-nanotubes composites, Synth Met. 103 (1999) 2510-2512.

[65] I.W. Frank, D.M. Tanenbaum, A.M. van der Zande, P.L. McEuen, Mechanical properties of suspended graphene sheets, Journal of Vacuum Science & Technology B: Microelectronics and Nanometer Structures. 25 (2007) 2558-2561.

[66] M. El Achaby, F.-. Arrakhiz, S. Vaudreuil, A. El Kacem Qaiss, M. Bousmina, O. Fassi-Fehri, Mechanical, thermal, and rheological properties of graphene-based polypropylene nanocomposites prepared by melt mixing, Polymer Composites. 33 (2012) 733-744.

[67] C. Bao, L. Song, W. Xing, B. Yuan, C.A. Wilkie, J. Huang, Y. Guo, Y. Hu, Preparation of graphene by pressurized oxidation and multiplex reduction and its polymer nanocomposites by masterbatch-based melt blending, Journal of Materials Chemistry. 22 (2012) 6088-6096.

[68] I.H. Kim, Y.G. Jeong, Polylactide/exfoliated graphite nanocomposites with enhanced thermal stability, mechanical modulus, and electrical conductivity, J. Polym. Sci. Part B. 48 (2010) 850-858.

[69] M. El Achaby, F.Z. Arrakhiz, S. Vaudreuil, E.M. Essassi, A. Qaiss, M. Bousmina, Preparation and characterization of melt-blended graphene nanosheets-poly(vinylidene fluoride) nanocomposites with enhanced properties, J Appl Polym Sci. 127 (2013) 4697-4707.

[70] H. Kim, S. Kobayashi, M.A. AbdurRahim, M.J. Zhang, A. Khusainova, M.A. Hillmyer, A.A. Abdala, C.W. Macosko, Graphene/polyethylene nanocomposites: Effect of polyethylene functionalization and blending methods, Polymer. 52 (2011) 1837-1846.

[71] X. An, T. Simmons, R. Shah, C. Wolfe, K.M. Lewis, M. Washington, S.K. Nayak, S. Talapatra, S. Kar, Stable aqueous dispersions of noncovalently functionalized graphene from graphite and their multifunctional high-performance applications, Nano Letters. 10 (2010) 4295-4301.

[72] K. Wakabayashi, P. Brunner, C. Pierre, S. Hewlett, J.M. Torkelson, Novel nanocomposites made from polymer and as-received, unmodified graphite: Effects of graphite level and dispersion on mechanical and electrical properties, crystallization, and thermal stability, AIChE Annual Meeting, Conference Proceedings. (2008).

[73] P. Steurer, R. Wissert, R. Thomann, R. Mülhaupt, Functionalized graphenes and thermoplastic nanocomposites based upon expanded graphite oxide, Macromolecular Rapid Communications. 30 (2009) 316-327.

[74] P. Song, Z. Cao, Y. Cai, L. Zhao, Z. Fang, S. Fu, Fabrication of exfoliated graphene-based polypropylene nanocomposites with enhanced mechanical and thermal properties, Polymer. 52 (2011) 4001-4010.

[75] C. Teng, C.M. Ma, C. Lu, S. Yang, S. Lee, M. Hsiao, M. Yen, K. Chiou, T. Lee, Thermal conductivity and structure of non-covalent functionalized graphene/epoxy composites, Carbon. 49 (2011) 5107-5116.

[76] Z. Mo, T. Xie, J. Zhang, Y. Zhao, R. Guo, Synthesis and Characterization of NanoGs-PPy/Epoxy Nanocomposites by In Situ Polymerization, Synthesis and Reactivity in Inorganic, Metal-Organic, and Nano-Metal Chemistry. 42 (2012) 1172-1176.

[77] S. Chatterjee, J.W. Wang, W.S. Kuo, N.H. Tai, C. Salzmann, W.L. Li, R. Hollertz, F.A. Nüesch, B.T.T. Chu, Mechanical reinforcement and thermal conductivity in expanded graphene nanoplatelets reinforced epoxy composites, Chemical Physics Letters. 531 (2012) 6-10.

[78] I. Zaman, H. Kuan, Q. Meng, A. Michelmore, N. Kawashima, T. Pitt, L. Zhang, S. Gouda, L. Luong, J. Ma, A Facile Approach to Chemically Modified Graphene and its Polymer Nanocomposites, Advanced Functional Materials. 22 (2012) 2735-2743.

[79] M.A. Rafiee, J. Rafiee, I. Srivastava, Z. Wang, H. Song, Z. Yu, N. Koratkar, Fracture and Fatigue in Graphene Nanocomposites, Small. 6 (2010) 179-183.

[80] J.R. Potts, S.H. Lee, T.M. Alam, J. An, M.D. Stoller, R.D. Piner, R.S. Ruoff, Thermomechanical properties of chemically modified graphene/poly(methyl methacrylate) composites made by in situ polymerization, Carbon. 49 (2011) 2615-2623.

[81] J.Y. Jang, M.S. Kim, H.M. Jeong, C.M. Shin, Graphite oxide/poly(methyl methacrylate) nanocomposites prepared by a novel method utilizing macroazoinitiator, Composites Sci. Technol. 69 (2009) 186-191.

[82] G. Chen, W. Weng, D. Wu, C. Wu, PMMA/graphite nanosheets composite and its conducting properties, European Polymer Journal. 39 (2003) 2329-2335.

[83] F.d.C. Fim, N.R.S. Basso, A.P. Graebin, D.S. Azambuja, G.B. Galland, Thermal, electrical, and mechanical properties of polyethylene–graphene nanocomposites obtained by in situ polymerization, J Appl Polym Sci. 128 (2013) 2630-2637.

[84] F. Zhang, X. Peng, W. Yan, Z. Peng, Y. Shen, Nonisothermal crystallization kinetics of in situ nylon 6/graphene composites by differential scanning calorimetry, Journal of Polymer Science Part B: Polymer Physics. 49 (2011) 1381-1388.

[85] Y. Pan, Z. Yu, Y. Ou, G. Hu, A new process of fabricating electrically conducting nylon 6/graphite nanocomposites via intercalation polymerization, J. Polym. Sci. B Polym. Phys. 38 (2000) 1626-1633.

[86] S.H. Lee, D.R. Dreyer, J. An, A. Velamakanni, R.D. Piner, S. Park, Y. Zhu, S.O. Kim, C.W. Bielawski, R.S. Ruoff, Polymer Brushes via Controlled, Surface-Initiated Atom Transfer Radical Polymerization (ATRP) from Graphene Oxide, Macromol. Rapid Commun. 31 (2010) 281-288.

[87] M. Fang, K. Wang, H. Lu, Y. Yang, S.Nutt, Covalent polymer functionalization of graphene nanosheets and mechanical properties of composites, J. Mater. Chem. (2009) 7098-7105.

[88] Y. Yang, J. Wang, J. Zhang, J. Liu, X. Yang, H. Zhao, Exfoliated Graphite Oxide Decorated by PDMAEMA Chains and Polymer Particles, Langmuir. 25 (2009) 11808-11814.

[89] V.K.S. Shante, S. Kirkpatrick, An introduction to percolation theory, Adv. Phys. 20 (1971) 325-357.

[90] J. Liang, Y. Wang, Y. Huang, Y. Ma, Z. Liu, J. Cai, C. Zhang, H. Gao, Y. Chen, Electromagnetic interference shielding of graphene/epoxy composites, Carbon. 47 (2009) 922-925.

[91] M. Monti, M. Rallini, D. Puglia, L. Peponi, L. Torre, J.M. Kenny, Morphology and electrical properties of graphene–epoxy nanocomposites obtained by different solvent assisted processing methods, Composites Part A. 46 (2013) 166-172.

[92] J. Li, J.K. Kim, M. Lung Sham, Conductive graphite nanoplatelet/epoxy nanocomposites: Effects of exfoliation and UV/ozone treatment of graphite, Scr. Mater. 53 (2005) 235-240.

[93] N. Liu, F. Luo, H. Wu, Y. Liu, C. Zhang, J. Chen, One-Step Ionic-Liquid-Assisted Electrochemical Synthesis of Ionic-Liquid-Functionalized Graphene Sheets Directly from Graphite, Adv. Funct. Mater. 18 (2008) 1518-1525.

[94] A.V. Raghu, Y.R. Lee, H.M. Jeong, C.M. Shin, Preparation and Physical Properties of Waterborne Polyurethane/Functionalized Graphene Sheet Nanocomposites, Macromol. Chem. Phys. 209 (2008) 2487-2493.

[95] H. Kim, C.W. Macosko, Processing-property relationships of polycarbonate/graphene composites, Polymer. 50 (2009) 3797-3809.

[96] H. Kim, C.W. Macosko, Morphology and Properties of Polyester/Exfoliated Graphite Nanocomposites, Macromolecules. 41 (2008) 3317-3327.

[97] S. Ansari, E.P. Giannelis, Functionalized graphene sheet—Poly(vinylidene fluoride) conductive nanocomposites, J. Polym. Sci. B Polym. Phys. 47 (2009) 888-897.

[98] T. Wei, G. Luo, Z. Fan, C. Zheng, J. Yan, C. Yao, W. Li, C. Zhang, Preparation of graphene nanosheet/polymer composites using in situ reduction–extractive dispersion, Carbon. 47 (2009) 2296-2299.

[99] M. Yoonessi, J.R. Gaier, Highly Conductive Multifunctional Graphene Polycarbonate Nanocomposites, ACS Nano. 4 (2010) 7211-7220.

[100] C. Wu, X. Huang, G. Wang, L. Lv, G. Chen, G. Li, P. Jiang, Highly Conductive Nanocomposites with Three-Dimensional, Compactly Interconnected Graphene Networks via a Self-Assembly Process, Advanced Functional Materials. 23 (2013) 506-513.

[101] K. Kalaitzidou, H. Fukushima, L.T. Drzal, A route for polymer nanocomposites with engineered electrical conductivity and percolation threshold, Materials. 3 (2010) 1089-1103.

[102] K. Kalaitzidou, H. Fukushima, L.T. Drzal, A new compounding method for exfoliated graphite-polypropylene nanocomposites with enhanced flexural properties and lower percolation threshold, Composites Sci. Technol. 67 (2007) 2045-2051.

[103] S. Kim, I. Do, L.T. Drzal, Multifunctional xGnP/LLDPE Nanocomposites Prepared by Solution Compounding Using Various Screw Rotating Systems, Macromol. Mater. Eng. 294 (2009) 196-205.

[104] W. Liu, I. Do, H. Fukushima, L. Drzal, Influence of processing on morphology, electrical conductivity and flexural properties of exfoliated graphite nanoplatelets-polyamide nanocomposties, Carbon letters. 11 (2010) 279-284.

[105] J. Ma, Q. Meng, A. Michelmore, N. Kawashima, Z. Izzuddin, C. Bengtsson, H. Kuan, Covalently bonded interfaces for polymer/graphene composites, J. Mater. Chem. A. (2013) 4255-4264.

[106] J. Hicks, A. Behnam, A. Ural, A computational study of tunneling-percolation electrical transport in graphene-based nanocomposites, Appl. Phys. Lett. 95 (2009) 213103.

[107] J. Li, J.K. Kim, Percolation threshold of conducting polymer composites containing 3D randomly distributed graphite nanoplatelets, Composites Sci. Technol. 67 (2007) 2114-2120.

[108] G. Eda, M. Chhowalla, Graphene-based Composite Thin Films for Electronics, Nano Lett. 9 (2009) 814-818.

[109] Y.B. Yi, E. Tawerghi, Geometric percolation thresholds of interpenetrating plates in three-dimensional space, Phys Rev E Stat Nonlin Soft Matter Phys. 79 (2009) 041134.

[110] S.H. - Munson-McGee, Estimation of the critical concentration in an anisotropic percolation network, Phys Rev B. 43 (1991) 3331-3336.

[111] I. Balberg, N. Binenbaum, Percolation thresholds in the three-dimensional sticks system, Phy Rev Lett. 52 (1984) 1465-1468.

[112] C. Li, E.T. Thostenson, T. Chou, Dominant role of tunneling resistance in the electrical conductivity of carbon nanotube–based composites, Appl. Phys. Lett. 91 (2007) 223114.

[113] Y. Yu, G. Song, L. Sun, Determinant role of tunneling resistance in electrical conductivity of polymer composites reinforced by well dispersed carbon nanotubes, J. Appl. Phys. 108 (2010) 084319.

[114] S. Geetha, K.K. Satheesh Kumar, C.R.K. Rao, M. Vijayan, D.C. Trivedi, EMI shielding: Methods and materials—A review, J Appl Polym Sci. 112 (2009) 2073-2086.

[115] J. Huang, EMI shielding plastics: A review, Adv. Polym. Technol. 14 (1995) 137-150.

[116] R. strümpler, J. Glatz-Reichenbach, FEATURE ARTICLE Conducting Polymer Composites, Journal of Electroceramics. 3 (1999) 329-346.

[117] Y. Dan, Y. Lu, N.J. Kybert, Z. Luo, A.T.C. Johnson, Intrinsic Response of Graphene Vapor Sensors, Nano Lett. 9 (2009) 1472-1475.

[118] J.T. Robinson, E.S. Snow, F.K. Perkins, Z. Wei, P.E. Sheehan, Reduced Graphene Oxide Molecular Sensors, Nano Letters. 8 (2008) 3137-3140.

[119] J. Liu, L. Tao, W. Yang, D. Li, C. Boyer, R. Wuhrer, F. Braet, T.P. Davis, Synthesis, Characterization, and Multilayer Assembly of pH Sensitive Graphene−Polymer Nanocomposites, Langmuir. 26 (2010) 10068-10075.

[120] L. Chen, G. Chen, L. Lu, Piezoresistive Behavior Study on Finger-Sensing Silicone Rubber/Graphite Nanosheet Nanocomposites, Adv. Funct. Mater. 17 (2007) 898-904.

[121] E. Yoo, J. Kim, E. Hosono, H. Zhou, T. Kudo, I. Honma, Large Reversible Li Storage of Graphene Nanosheet Families for Use in Rechargeable Lithium Ion Batteries, Nano Letters. 8 (2008) 2277-2282.

[122] H. Gómez, M.K. Ram, F. Alvi, P. Villalba, E.(. Stefanakos, A. Kumar, Graphene-conducting polymer nanocomposite as novel electrode for supercapacitors, Journal of Power Sources. 196 (2011) 4102-4108.

[123] K. Zhang, L.L. Zhang, X.S. Zhao, J. Wu, Graphene/Polyaniline Nanofiber Composites as Supercapacitor Electrodes, Chem. Mater. 22 (2010) 1392-1401.

[124] Q. Wu, Y. Xu, Z. Yao, A. Liu, G. Shi, Supercapacitors Based on Flexible Graphene/Polyaniline Nanofiber Composite Films, ACS Nano. 4 (2010) 1963-1970.

[125] G. Eda, Y. Lin, S. Miller, C. Chen, W. Su, M. Chhowalla, Transparent and conducting electrodes for organic electronics from reduced graphene oxide, Appl. Phys. Lett. 92 (2008) 233305.

[126] J. Wu, H.A. Becerril, Z. Bao, Z. Liu, Y. Chen, P. Peumans, Organic solar cells with solution-processed graphene transparent electrodes, Appl. Phys. Lett. 92 (2008) 263302.

[127] X. Wang, L. Zhi, K. Müllen, Transparent, Conductive Graphene Electrodes for Dye-Sensitized Solar Cells, Nano Letters. 8 (2008) 323-327.

[128] G.L. POLLACK, Kapitza resistance, Rev. Mod. Phys. 41 (1969) 48-81.

[129] H. Zhong, J.R. Lukes, Interfacial thermal resistance between carbon nanotubes: molecular dynamics simulations and analytical thermal modeling, Phy. Rev. B. 74 (2006) 125403-125413.

[130] S.H. Xie, Y.Y. Liu, J.Y. Li, Comparison of the effective conductivity between composites reinforced by graphene nanosheets and carbon nanotubes, Appl. Phys. Lett. 92 (2008) 243121.

[131] S. Ghose, D.C. Working, J.W. Connell, J.G. Smith Jr., K.A. Watson, D.M. Delozier, Y.P. Sun, Y. Lin, Thermal conductivity of UltemTM/carbon nanofiller blends, High Perform. Polymers. 18 (2006) 961-977.

[132] S. Yang, W. Lin, Y. Huang, H. Tien, J. Wang, C.M. Ma, S. Li, Y. Wang, Synergetic effects of graphene platelets and carbon nanotubes on the mechanical and thermal properties of epoxy composites, Carbon. 49 (2011) 793-803.

[133] S. Ganguli, A.K. Roy, D.P. Anderson, Improved thermal conductivity for chemically functionalized exfoliated graphite/epoxy composites, Carbon. 46 (2008) 806-817.

[134] X. Sun, P. Ramesh, M.E. Itkis, E. Bekyarova, R.C. Haddon, Dependence of the thermal conductivity of two-dimensional graphite nanoplatelet-based composites on the nanoparticle size distribution, J. Phys. : Condens. Matter. 22 (2010) 334216.

[135] K.M.F. Shahil, A.A. Balandin, Graphene–Multilayer Graphene Nanocomposites as Highly Efficient Thermal Interface Materials, Nano Lett. 12 (2012) 861-867.

[136] K. Kalaitzidou, H. Fukushima, L.T. Drzal, Multifunctional polypropylene composites produced by incorporation of exfoliated graphite nanoplatelets, Carbon. 45 (2007) 1446-1452.

[137] H. Fukushima, L.T. Drzal, B.P. Rook, M.J. Rich, Thermal conductivity of exfoliated graphite nanocomposites, Journal of Thermal Analysis and Calorimetry. 85 (2006) 235-238.

[138] K.M.F. Shahil, A.A. Balandin, Thermal properties of graphene and multilayer graphene: Applications in thermal interface materials, Solid State Communications. 152 (2012) 1331-1340.

[139] H.J. Salavagione, M.A. Gómez, G. Martínez, Polymeric modification of graphene through esterification of graphite oxide and poly(vinyl alcohol), Macromolecules. 42 (2009) 6331-6334.

[140] Y. Xu, W. Hong, H. Bai, C. Li, G. Shi, Strong and ductile poly(vinyl alcohol)/graphene oxide composite films with a layered structure, Carbon. 47 (2009) 3538-3543.

[141] S. Villar-Rodil, J.I. Paredes, A. Martínez-Alonso, J.M.D. Tascón, Preparation of graphene dispersions and graphene-polymer composites in organic media, Journal of Materials Chemistry. 19 (2009) 3591-3593.

[142] T. Kashiwagi, F. Du, J.F. Douglas, K.I. Winey, R.H. Harris Jr., J.R. Shields, Nanoparticle networks reduce the flammability of polymer nanocomposites. Nature materials. 4 (2005) 928-933.

[143] J.A. King, D.R. Klimek, I. Miskioglu, G.M. Odegard, Mechanical properties of graphene nanoplatelet/epoxy composites, J Appl Polym Sci. (2012).

[144] M.A. Rafiee, J. Rafiee, Z. Wang, H. Song, Z. Yu, N. Koratkar, Enhanced mechanical properties of nanocomposites at low graphene content, ACS Nano. 3 (2009) 3884-3890.

[145] S. Araby, A. Maged, I. Zaman, J. Ma, P. Majewski, A facile approach to fabricate elastomer/graphene platelets nanocomposites, Proceedings of SPIE - The International Society for Optical Engineering. 8793 (2013).

[146] D.R. Paul, L.M. Robeson, Polymer nanotechnology: Nanocomposites, Polymer. 49 (2008) 3187-3204.

CHAPTER 3： Production of Few-Layer Graphene by Direct Exfoliation of Graphite in Liquid Phase

3.1 Introduction

Since the discovery of graphene in 2004 by micromechanical exfoliation [1], several routes have been developed to produce graphene. Based on the quality and quantity, graphene produced by different methods is used for various applications. For instance, high quality single-layer graphene produced by micromechanical exfoliation and CVD is available in very limited quantities and is only suitable for fundamental study or for electronic applications [2,3]. The exfoliation and reduction of graphite oxide (GO) can produce graphene on large scale. However, the use of hazardous chemicals during the oxidation and reduction processes makes this approach neither safe nor environmental friendly. More importantly, it has been reported that the oxidation process introduces structural defects into pristine graphene sheets [4,5]. A new production technique for high quality graphene, the direct exfoliation of graphite in liquid phase, was first introduced by Coleman et al. in 2008 [6]. Graphite powder can be dispersed and exfoliated in N-methyl-pyrrolidone (NMP), due to the matching surface energies of the graphite and the solvent. Inspired by the pioneering work done by Coleman and coworkers, many researchers have concentrated their efforts on the development of liquid phase production of graphene. There are three types of liquids that have the ability to exfoliate graphite into graphene: organic solvents [7-9] , surfactant/water solutions [10-12], and ionic liquids

[13,14].

NMP, the most widely used solvent for the exfoliation of graphene, has been identified as toxic for the reproductive system; inhalation and dermal exposure to NMP must be carefully limited [15]. Also, it is difficult to scale up the production using ionic liquid because of its high price. Finally, for most traditional surfactant/water systems, the final products are graphene films obtained by vacuum filtration of the well-sonicated dispersions, and the residue of the surfactant in those films has been demonstrated to hamper the contact between graphene sheets, thus reducing the electrical conductivities [16].

In this work, Gum Arabic (GA) is employed as a non-ionic surfactant to assist in the exfoliation of graphite in water. GA is a water soluble natural polymer, mainly composed of highly branched polysaccharide, with a molecular weight of 250000[17]. It has been suggested that the minor but important component, protein–polysaccharide complex, contributes to the strong emulsification and stabilization properties of GA [18]. Due to its special structure and properties, GA has previously been used to unbundle and stabilized carbon nanotubes in aqueous solutions. GA has proven better than many other surfactants at dispersing carbon nanomaterials [19]. Similarly, it is believed that GA can be used to exfoliate graphite due to the same Van der Waals interactions between individual nanotubes and graphene sheets. Other reasons for choosing GA include its relatively low cost and the minimal safety concerns surrounding it, as demonstrated by extensive applications in the food industry, for example with candies, chewing gum and carbonated beverages. Uniquely, in this work, several grams of pure graphene powder was produced

in one batch, due to the high dispersion concentration of graphene and to the additional acid hydrolysis treatment employed after sonication, in order to remove GA.

3.2 Materials and Methods

3.2.1 Production of Graphene Dispersion with Gum Arabic

Three different sizes of graphite (2-15 μm, 44 μm and 2000 μm) purchased from Alfa Aesar were used as the starting material, without any further treatments. Based on the size, three different kinds of parent graphite were donated as G-S, G-M and G-L. Corresponding graphene products were named g-S, g-M and g-L, respectively. G-S and G-M were black-grey fine powders, while G-L consisted of flakes with metallic shininess. Quantitative gum Arabic (Sigma) was first dissolved in 2L of distilled water and sonicated for 1 hour, to make a 2 wt.% solution. Then, 50g of graphite was added into the well-dissolved gum Arabic solution. Graphene dispersion was obtained by ultrasonication in a low power sonication bath (Fisher Scientific，FS220，40KHz) for 60 hours. The sonication bath was operated 8 hours per day and the time was carefully recorded.

3.2.2 Acid hydrolysis treatment

To totally remove the GA, the graphene/GA mixture obtained was left undisturbed for 24 hours to precipitate the un-exfoliated graphite. The supernatant was decanted into another beaker and underwent volume reduction by mild heating and stirring. The

graphene/GA mixture was then dispersed in 200 mL of nitric acid (70 wt.%, Fisher Chemical) in a 500 mL round bottom flask equipped with a condenser and the dispersion was refluxed under magnetic stirring for 6 hours. The resulting dispersion was diluted with distilled water and filtered. The filter cake obtained was washed several times until a neutral pH was achieved. Finally, the cake was re-dispersed in a small amount of water and freeze dried to get pure graphene powder.

3.3 Results and Discussions

3.3.1 Thermal Gravimetric Analysis (TGA)

For most surfactant assisted exfoliation methods, the final products are just graphene dispersions or graphene films mixed with surfactants obtained by vacuum filtration. Further purifications are usually not applied. It is important to produce surfactant-free dry graphene powder for subsequent applications such as the production of nanocomposites. Thermal gravimetric analysis（TGA）was used to confirm the purity of the graphene powder. Graphene samples were heated up to 950℃, with a slow rate of 5℃/min under airflow. As shown in Figure 3-1, there is only one graphitic peak at 750℃ in the differential temperature curve (blue line), which means that all of the gum Arabic is successfully removed, and the graphene product is ready for any desired application. However, before the application of acid hydrolysis treatment, the TGA results show a 2-stage mass loss (Figure 3-2). The first one occurs between 200℃ and 400℃ and can be attributed to the decomposition of GA[18]. The weight of the residual GA is estimated

as significant at 23%.

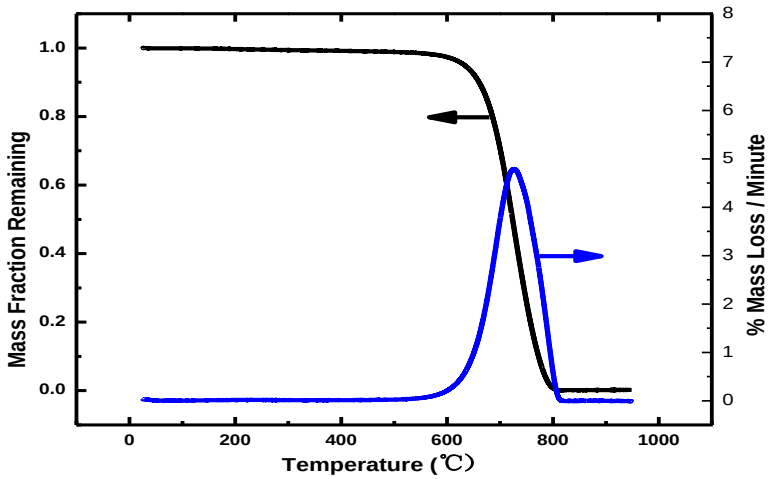

Figure 3-1 TGA curve of purified graphene

.

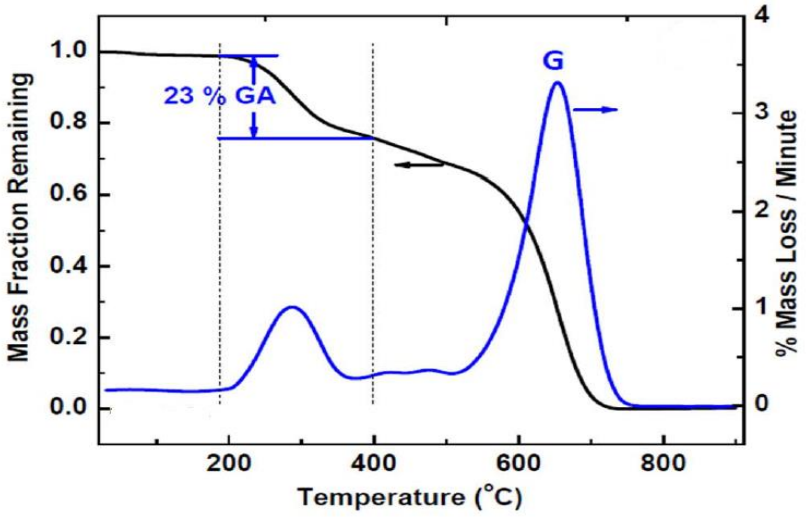

Figure 3-2 TGA curve of un-purified graphene

3.3.2 Raman Spectroscopy

Since 2006, the Raman spectroscopy has become an essential characterization method for graphene materials [20]. The electronic structure of graphene can be uniquely detected by the Raman spectroscopy, and it is nondestructive and high-throughput. There are three main characteristic peaks in the Raman spectroscopy of graphene, including a G peak at ~1580 cm^{-1}, a D peak at ~1350 cm^{-1} and a D peak second order, namely 2D peak at ~2700 cm^{-1}. The most important capacity of the Raman is the identification of the number of graphene layers, which is based on the shape, width, and position changes of the 2D peak. Figure 3-3 shows the evolution of the 2D peak from graphite to single-layer graphene [20]. The 2D peak is red-shifted with a reducing number of graphene layers and a single sharp peak is observed for mono-layer graphene. The Raman spectroscopies of graphene produced by different sizes of parent graphite are presented in Figure 3-4. These results suggest that the as-produced graphene samples consist of few-layer graphene (approximately 5 layers).

The Raman spectroscopy is also able to investigate the defect concentration of graphene, which is associated with the D peak. The appearance of the D peak and the relative intensity to that of the G peak (I_D /I_G) represent the disorder of the graphitic structure. For defect-free graphite, the D peak can be ignored compared to the intense G peak [21]. After the mild exfoliation process, the defect ratios of graphene remain at significantly low values. The estimated defect ratios of as-produced graphene, graphene synthesized by other liquid phase exfoliation methods, and the chemical reduction of GO (r-GO) are summarized in Table 3-1. It is clear that the defect ratios of as-produced graphene increase when increasing the size of parent graphite. As expected, all of them

are much lower than those obtained for reduced GO, owing to the non-oxidative mild exfoliation process. Interestingly, compared to other liquid phase exfoliation processes, the defect ratios for as-produced samples are still considerably lower. The results indicated that the pristine graphitic structure is successfully preserved, and only a few defects were introduced to the basal plane after this mild but effective exfoliation process. Gum Arabic adsorbs to the surface of graphite, providing a strong emulsification property and assisting the exfoliation process of graphite.

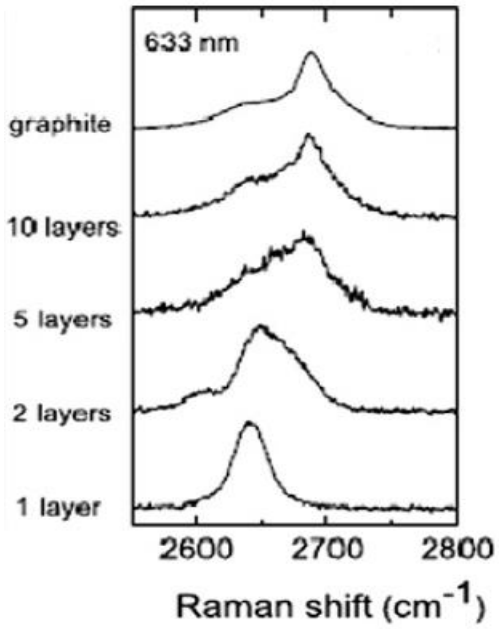

Figure 3-3 Evolution of 2D peak with increasing number of layers [20]

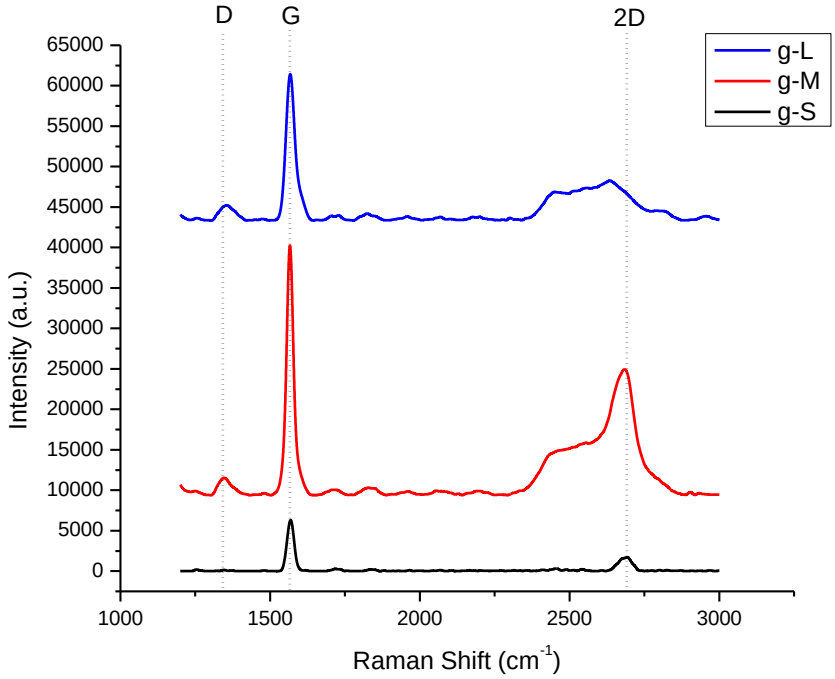

Figure 3-4 Raman spectroscopies of three kinds of graphene

Table 3-1 Summary of defect ratios

Material	Defect Ratio(I_D/I_G)	Reference
G (2-15 μ m)	~ 0	
G (44 μ m)	0.07	
G (2000 μ m)	0.1	
Exfoliated G	0.3-1.4	[22-24]
Reduced GO	1.31	[25]

3.3.3 Microscopies

Scanning electron microscope (SEM) was used to investigate the morphology and size of exfoliated graphene. A small amount of dry graphene powder was loaded onto carbon tape for SEM characterization. Representative images of g-S, g-M and g-L are shown in Figure 3-5-A, B and C. The flakes of all three types of graphene appear to be flat and rigid in contrast to the wrinkled sheet morphology discovered for reduced GO [25], whereas similar to the morphology of graphene nanoplatelets produced by the intercalation of small molecules and exfoliation [26]. The smooth surface texture indicates that all flakes are mostly free of plane defects. However, the edges of g-L are observed to be not as sharp and well-defined as those of g-S and g-M, which is in agreement with the relatively greater number of edge defects of g-L illustrated by Raman. From the SEM analysis, it is shown that all samples produced by liquid phase exfoliation exhibit polydispersity in terms of sheet dimension and thickness. Lateral size varies widely from a few hundred nanometers to a few microns, and thickness (number of layers) is not uniform either. Although most of the flakes are very thin and appear to be semi-transparent, some thick aggregations are easily observed especially in the case of g-L. These are inevitable drawbacks of the liquid phase production of graphene due to the uncontrollable sonication force.

Transmission electron microscopy (TEM) was used for further investigation of size and thickness. TEM sample was prepared by re-dispersing a tiny amount of graphene and dropping the dispersion onto a carbon-coated copper grid. The selected images for g-S,

g-M and g-L are presented in Figures 3-5-a, b and c, respectively. Thanks to the higher resolution of TEM, we are able to have a closer and clearer look at the graphene sheet. Thin graphene flakes are stacked together or folded into many clusters with a lateral size of a few hundred nanometers. Each cluster consists of a large number of disordered flat sheets. Smaller and more disordered sheets are observed for the cluster of g-L, making it look blurrier than the other two samples. The well-defined edges of g-S and g-M allow a clear distinction between sheets and all the observed sheets are of good quality with no visible damages such as holes or cracks. Single-, bi-, and multi-layered graphene can be clearly identified based on the color contrast within one cluster.

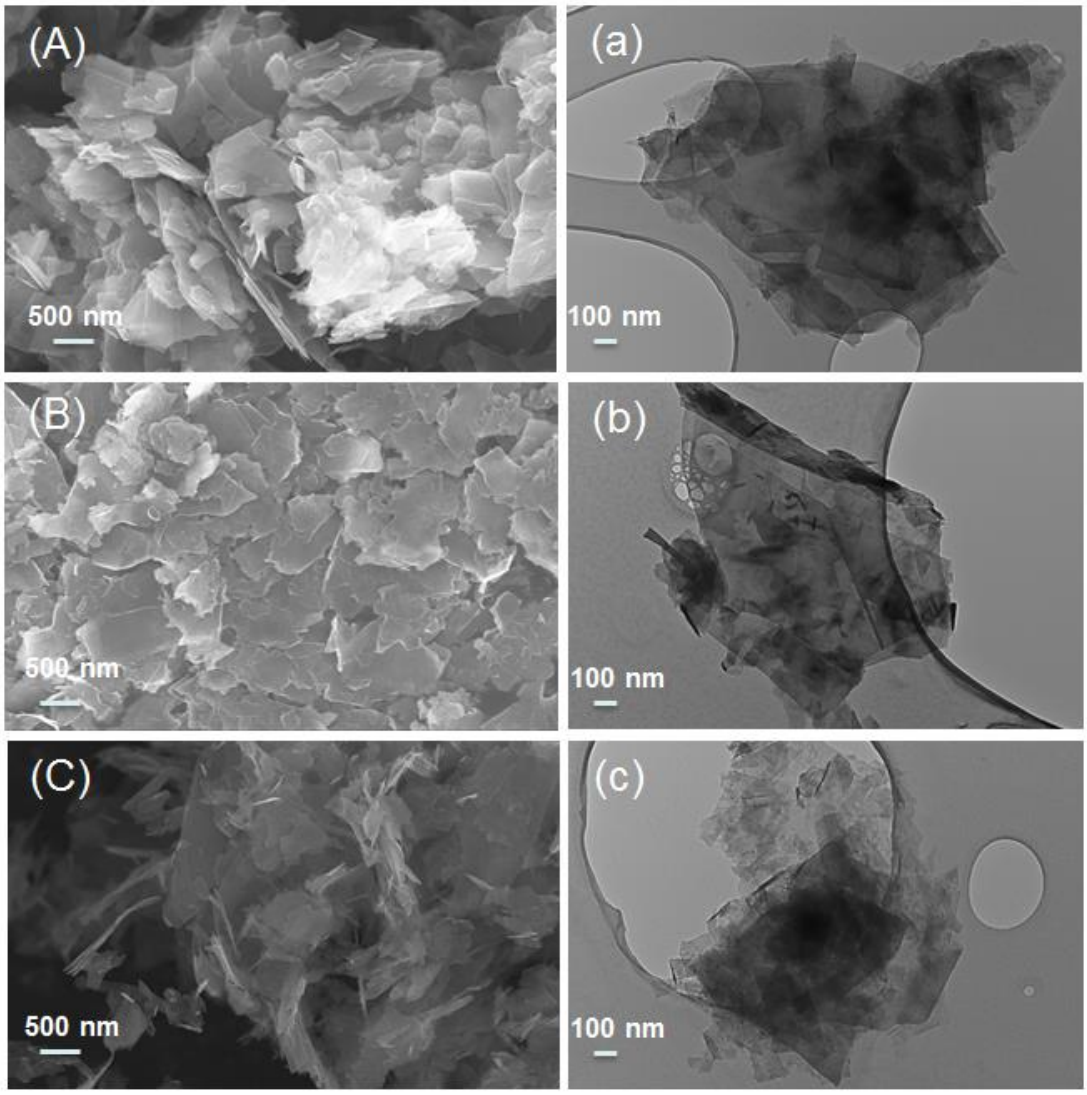

Figure 3-5 SEM images of (A): g-S, (B): g-M and (C): g-L; TEM images for (a): g-S, (b): g-M, (c): g-L

3.3.4 Electrical Conductivity

Since using graphene as a conductive filler for polymer nanocomposites is one of our target applications, it is important to measure the intrinsic conductivity of graphene. To measure the conductivity of graphene, a small amount of powder was first pressed into a thin pellet at 4000 psi, to ensure the best contact of the material. Electrical

conductivity was measured by placing the pellet into a custom four-probe stage with 1.5 mm spacing, connected to a multi-channel electrochemical testing platform. Figure 3-6 demonstrates the comparison of average electrical conductivities for as-produced graphene, R-GO, and graphene produced by other surfactant assisted liquid-phase exfoliation methods from literatures [10,25,27]. To be noted, for example, g-Brij700 indicates that the surfactant used for this method is Brij700 and the conductivity is measured for the film obtained after vacuum filtration. Conductivities for as-produced graphene are in the range from 235.2 to 280.9 S/cm, with a positive correlation to the size of the parent graphite. Because of the fewer defects introduced by liquid phase exfoliation process, as previously discussed, conductivities of 40 times higher than those of regularly produced r-GO are obtained. Although additional treatment can be applied to increase the degree of reduction and conductivity of r-GO to approach our range, the process will become inefficient and costly. The superior electrical properties found for as-produced graphene when compared to other liquid phase exfoliation methods can be attributed to the unique surfactant purification step. The highly conductive purified graphene powder has a great potential to enhance the electrical property of nanocomposites once incorporated into the polymer matrix.

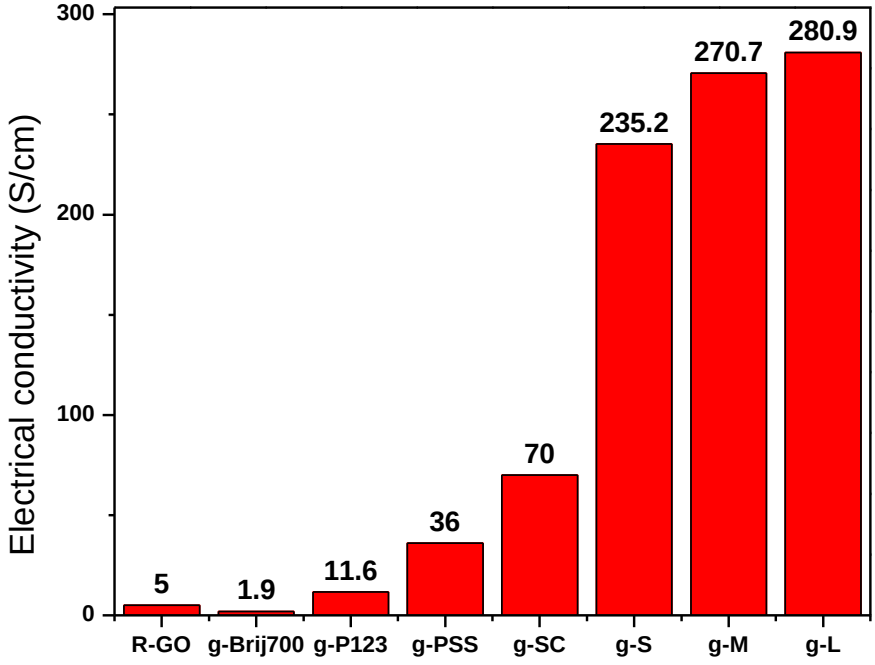

Figure 3-6 Comparison of conductivities of various graphene

3.3.5 Yield of Production

One of the most significant limitations of the liquid phase production of graphene is the low dispersion concentration and the low yield of production. Currently, based on different exfoliation systems and conditions employed, concentrations of graphene dispersions are in the range of 0.01mg/mL to 5.33mg/mL [16]. In this work, comparable results were achieved. For different starting graphite materials, the concentrations are 2.85mg/mL, 1.85mg/mL and 0.6mg/mL for G-S, G-M and G-L respectively. When all other conditions are identical, the graphite with smaller size seems to respond better to exfoliation in the solution, which can be interpreted as the highly specific surface area of

a small particle better exploiting the ultrasound power. The ultrasound energy generated by the formation, growth and collapse of the cavitation bubbles surrounds the small particle, inducing more exfoliation. Although the concentration of the dispersions are not extremely high, by boosting the starting mass of graphite to 50g and the volume of the reaction vessel to 2L, a considerable quantity of dry graphene powder product is obtained for each batch, specifically, 5.7g for g-S, 3.7g for g-M and 1.2g for g-L. Based on the mass of the starting graphite, the yields of few-layer graphene are 11.4%, 7.4% and 2.4%. The un-exfoliated mass could be collected and re-dispersed to further increase the overall yield.

3.4 Conclusions

In conclusion, a simple, green, and cost-effective route to producing few-layer graphene in a gum Arabic aqueous solution by physical sonication has been developed. Owing to the additional purification and freeze-drying processes, the product of the liquid phase exfoliation method is presented in the form of 100% pure dry powder for the first time ever. Three starting graphite materials in different sizes were studied, and the products obtained were analyzed by a combination of spectroscopy and microscopy techniques. Graphene produced from all three graphite possess high quality sheets, almost free of defects, and with high electrical conductivities. No significant impact of parent graphite size has been discovered on the quality of graphene. The only disadvantage is that the yield for g-L is relatively low. Although it has slightly higher conductivity, it is

not promising for polymer nanocomposite applications because of the insufficiency. The capacities of our products for electrical property enhancements in polymer nanocomposites will be discussed in the next chapter.

References

[1] K.S. Novoselov, A.K. Geim, S.V. Morozov, D. Jiang, Y. Zhang, S.V. Dubonos, I.V. Grigorieva, A.A. Firsov, Electric Field Effect in Atomically Thin Carbon Films, Science. 306 (2004) 666-669.

[2] P.R. Somani, S.P. Somani, M. Umeno, Planer nano-graphenes from camphor by CVD, Chemical Physics Letters. 430 (2006) 56-59.

[3] A. Reina, X. Jia, J. Ho, D. Nezich, H. Son, V. Bulovic, M.S. Dresselhaus, K. Jing, Large area, few-layer graphene films on arbitrary substrates by chemical vapor deposition, Nano Letters. 9 (2009) 30-35.

[4] H.A. Becerril, J. Mao, Z. Liu, R.M. Stoltenberg, Z. Bao, Y. Chen, Evaluation of solution-processed reduced graphene oxide films as transparent conductors, ACS Nano. 2 (2008) 463-470.

[5] H.C. Schniepp, J. Li, M.J. McAllister, H. Sai, M. Herrera-Alonso, D.H. Adamson, R.K. Prud'homme, R. Car, D.A. Saville, I.A. Aksay, Functionalized Single Graphene Sheets Derived from Splitting Graphite Oxide, The Journal of Physical Chemistry B. 110 (2006) 8535-8539.

[6] Y. Hernandez, V. Nicolosi, M. Lotya, F.M. Blighe, Z. Sun, S. De, I.T. McGovern, B. Holland, M. Byrne, Y.K. Gun'Ko, J.J. Boland, P. Niraj, G. Duesberg, S. Krishnamurthy, R. Goodhue, J. Hutchison, V. Scardaci, A.C. Ferrari, J.N. Coleman, High-yield production of graphene by liquid-phase exfoliation of graphite, Nature Nanotechnology. 3 (2008) 563-568.

[7] E. Choi, W.S. Choi, Y.B. Lee, Y. Noh, Production of graphene by exfoliation of graphite in a volatile organic solvent, Nanotechnology. 22 (2011) 365601.

[8] U. Khan, H. Porwal, A. O'Neill, K. Nawaz, P. May, J.N. Coleman, Solvent-Exfoliated Graphene at Extremely High Concentration, Langmuir. 27 (2011) 9077-9082.

[9] M. Yi, Z. Shen, S. Ma, X. Zhang, A mixed-solvent strategy for facile and green preparation of graphene by liquid-phase exfoliation of graphite, J Nanopart Res. 14 (2012) 1-9.

[10] M. Lotya, P.J. King, U. Khan, S. De, J.N. Coleman, High-Concentration, Surfactant-Stabilized Graphene Dispersions, ACS Nano. 4 (2010) 3155-3162.

[11] M. Lotya, Y. Hernandez, P.J. King, R.J. Smith, V. Nicolosi, L.S. Karlsson, F.M. Blighe, S. De, Z. Wang, I.T. McGovern, G.S. Duesberg, J.N. Coleman, Liquid Phase

Production of Graphene by Exfoliation of Graphite in Surfactant/Water Solutions, J. Am. Chem. Soc. 131 (2009) 3611-3620.

[12] M. Zhang, R.R. Parajuli, D. Mastrogiovanni, B. Dai, P. Lo, W. Cheung, R. Brukh, P.L. Chiu, T. Zhou, Z. Liu, E. Garfunkel, H. He, Production of Graphene Sheets by Direct Dispersion with Aromatic Healing Agents, Small. 6 (2010) 1100-1107.

[13] X. Wang, P.F. Fulvio, G.A. Baker, G.M. Veith, R.R. Unocic, S.M. Mahurin, M. Chi, S. Dai, Direct exfoliation of natural graphite into micrometre size few layers graphene sheets using ionic liquids, Chem. Commun. 46 (2010) 4487-4489..

[14] D. Nuvoli, High concentration few-layer graphene sheets obtained by liquid phase exfoliation of graphite in ionic liquid, Journal of materials chemistry. 21 (2011) 3428-3431.

[15] T.S. Poet, C.R. Kirman, M. Bader, C. van Thriel, M.L. Gargas, P.M. Hinderliter, Quantitative Risk Analysis for N-Methyl Pyrrolidone Using Physiologically Based Pharmacokinetic and Benchmark Dose Modeling, Toxicological Sciences. 113 (2010) 468-482.

[16] W. Du, X. Jiang, L. Zhu, W. Du, X. Jiang, L. Zhu, From graphite to graphene: direct liquid-phase exfoliation of graphite to produce single- and few-layered pristine graphene, Journal of Materials Chemistry A. 1 (2013) 10592-10606.

[17] H.A. Swenson, H.M. Kaustinen, O.A. Kaustinen, N.S. Thompson, H.A. Swenson, H.M. Kaustinen, O.A. Kaustinen, N.S. Thompson, Structure of gum arabic and its configuration in solution, Journal of Polymer Science Part A?2: Polymer Physics. 6 (1968) 1593-1606.

[18] Y. Dror, Y. Cohen, R. Yerushalmi ‐ rozen, Y. Dror, Y. Cohen, R. Yerushalmi ‐ rozen, Structure of gum arabic in aqueous solution, Journal of Polymer Science Part B: Polymer Physics. 44 (2006) 3265-3271.

[19] R. Bandyopadhyaya, E. Nativ-Roth, O. Regev, R. Yerushalmi-Rozen, Stabilization of Individual Carbon Nanotubes in Aqueous Solutions, Nano Letters. 2 (2002) 25-28.

[20] A.C. Ferrari, M., A.C. Ferrari, J.C. Meyer, V. Scardaci, C. Casiraghi, M. Lazzeri, F. Mauri, S. Piscanec, D. Jiang, K.S. Novoselov, S. Roth, A.K. Geim, Raman spectrum of graphene and graphene layers, Phys. Rev. Lett. (2006).

[21] F. Tuinstra, J.L. Koenig, Raman Spectrum of Graphite, J. Chem. Phys. 53 (1970) 1126-1130.

[22] U. Khan, A. O'Neill, M. Lotya, S. De, J.N. Coleman, High-Concentration Solvent Exfoliation of Graphene, Small. 6 (2010) 864-871.

[23] M. Lotya, Y. Hernandez, P.J. King, R.J. Smith, V. Nicolosi, L.S. Karlsson, F.M. Blighe, S. De, Z. Wang, I.T. McGovern, G.S. Duesberg, J.N. Coleman, Liquid Phase Production of Graphene by Exfoliation of Graphite in Surfactant/Water Solutions, J. Am. Chem. Soc. 131 (2009) 3611-3620.

[24] J.T. Seo, A.A. Green, A.L. Antaris, M.C. Hersam, High-Concentration Aqueous Dispersions of Graphene Using Nonionic, Biocompatible Block Copolymers, J. Phys. Chem. Lett. 2 (2011) 1004-1008.

[25] V. Chabot, B. Kim, B. Sloper, C. Tzoganakis, A. Yu, High yield production and purification of few layer graphene by Gum Arabic assisted physical sonication, Science Reports. 3 (2013).

[26] A. Yu, P. Ramesh, M.E. Itkis, E. Bekyarova, R.C. Haddon, Graphite Nanoplatelet-Epoxy Composite Thermal Interface Materials, Journal of Physical Chemistry C. 111 (2007) 7565-7569.

[27] L. Guardia, M.J. Fernández-Merino, J.I. Paredes, P. Solís-Fernández, S. Villar-Rodil, A. Martínez-Alonso, J.M.D. Tascón, High-throughput production of pristine graphene in an aqueous dispersion assisted by non-ionic surfactants, Carbon. 49 (2011) 1653-1662.

CHAPTER 4：Preparation of Electrically Conductive Epoxy/Graphene Nanoplatelet Nanocomposites

4.1 Introduction

Incorporating electrical conductive fillers into polymeric resins can make conductive composites. A conductive pathway is formed when a sufficient quantity of conducting filler is dispersed into a polymer matrix. Silver nanoparticles have been extensively studied as fillers for electrically conductive composites or adhesives, because of their high intrinsic conductivities. However, high filler-loadings of up to 70 wt.% are usually required for metallic fillers [1-3], which in turn can result in poor mechanical properties, increase the density of the materials and increase the difficulties of processing. Nano-sized carbon materials such as carbon black (CB) and carbon nanotube (CNT) are also popular fillers for conductive nanocomposites, whereas the zero-dimensional spherical shape of CB tends to aggregate in polymer matrices and increase the volume resistivity [4]. CNTs can effectively form conductive pathways within polymer matrices at relatively low loadings, while the high cost has limited its practical application in industrial fields [5]. The discovery and rapid development of synthesis methods of graphene have created a new class of fillers for conductive nanocomposites. The two-dimensional flake-like material has several advantages that are ideal for conductive nanocomposite applications including high conductivity, high surface area and aspect ratio, compatibility with various polymer matrices, and cost effectiveness.

Electrically conductive polymer nanocomposites are primarily used for electromagnetic interference (EMI) shielding and electrostatic dissipation (ESD). Conductivity requirements are greater than 0.01 S/cm and 10^{-6}-10^{-2} S/cm for EMI and ESD, respectively [6]. EMI shielding is crucial for the protection of electronic devices from both incoming and outgoing electromagnetic waves. The enclosures of devices must be electrically conductive to ensure their proper functioning. Although most polymers are insulated, polymers with appropriate modifications surpass conventional metal-based EMI shielding materials in terms of weight, corrosion resistance, processability, and cost. Two strategies are commonly used for modifications: coating or blending with conductive fillers. Blending with conductive fillers, as known as fabricating nanocomposites, is more promising than coating techniques, especially as electronic devices are becoming smaller in size and more complicated in geometry [7].

Epoxies are typical thermosetting resins widely used as adhesives, coatings, and structural materials. They have also been extensively studied as matrices for nanocomposites due to their relatively low viscosities, compatibilities with various types of fillers, and ease of processing. Generally, nanocomposites based on epoxies are fabricated by the combination of in-situ polymerization and solution blending. Proper organic solvents that are compatible with both epoxy and fillers are necessary to obtain better states of dispersion. However, solvents must be totally removed before the curing step, and the prevention of the re-aggregation of filler during solvent removal is one of the major concerns about this kind of procedure. Solvents are regularly slowly removed

by heating and magnetic stirring. A novel hot sonication technique was introduced to reduce the chance of re-aggregation and was compared to regular solvent removal method.

In terms of conducting fillers, the self-produced liquid phase exfoliated graphene was first examined. Although the high conductivity, low-defect structure, and high scale of production all indicated that liquid phase exfoliated graphene was a promising source for the enhancement of the electrical property of nanocomposite, the results were not as good as expected. Consequently, in order to make electrically conductive composites, commercially available graphene nanoplatelets (xGnP) consequently drew our attention. xGnPs were carefully compared with as-produced liquid-phase exfoliated graphene, and were used for further studies, including the effect of filler size, the efficiency of hot sonication technique and the synergistic effect with a one-dimensional filler.

4.2Materials and Methods

4.2.1 Fillers

The graphene fillers studied in this work the three kinds of liquid-phase exfoliated graphene produced in Chapter 3 and four different grades of graphene nanoplatelets (xGnP) purchased from XG Sciences (Lansing, MI, USA). The specifications of the four types of xGnP are summarized in Table 4-1. The aspect ratio was calculated as the diameter divided by the thickness. xGnP powder was pressed into small pellet at 4000 psi

and subjected to electrical conductivity testing. Although C-300 and C-750 power were too rigid to be pressed into pellets, it's reasonable to believe that the conductivities are similar to those of M-5 and M-25. Other specifications were obtained from the supplier.

Table 4-1 Specifications of four types of xGnPs

Type	**Thickness (nm)**	**Diameter (μm)**	**Surface Area (m^2/g)**	**Aspect Ratio (D/T)**	**Electrical Conductivity (S/cm)**
C-750	2	1	750	500	~
M-5	6	5	150	833	648.6
C-300	2	2	300	1000	~
M-25	6	25	120	4167	739.6

Scanning electron microscope (SEM) images of the four types of xGnP at the same magnification are shown in Figure 4-1.

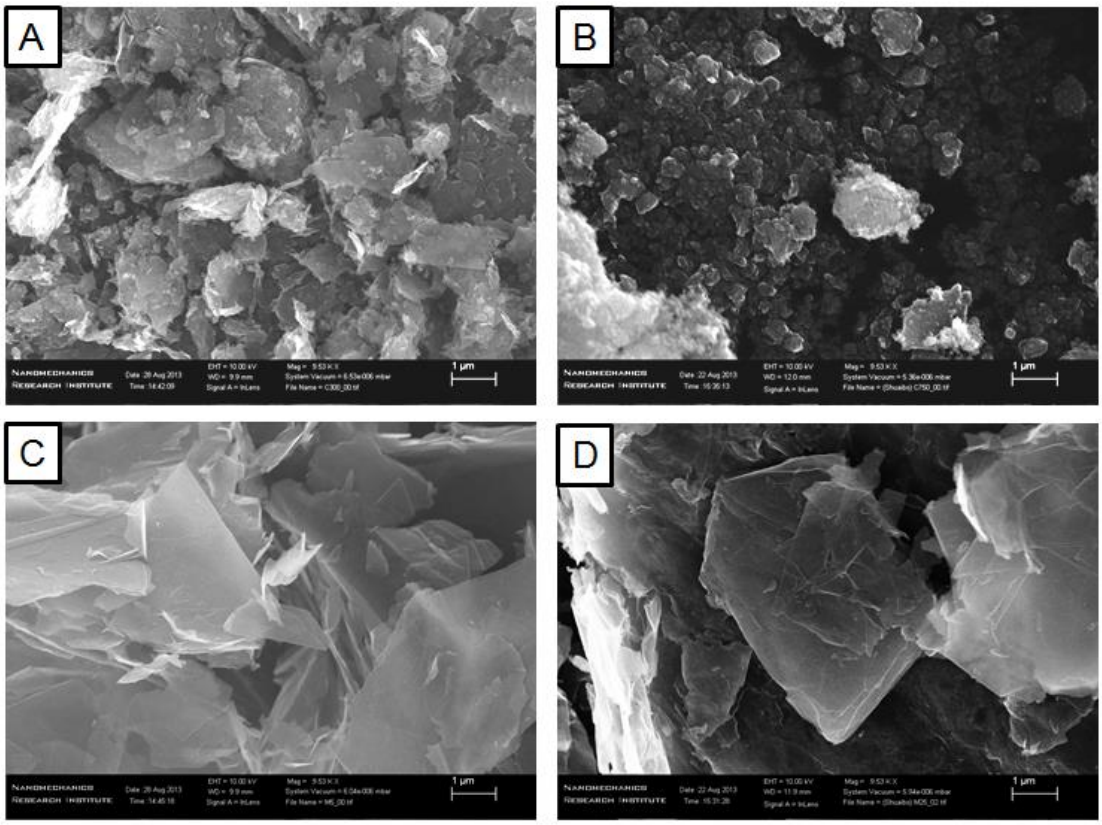

Figure 4-1 Specifications of four types of xGnP A: C-300, B: C-750, C: M-5, D: M-25

From the SEM images above (Figure 4-1), it is clear that all four types of xGnP have 2-D platelet shapes, and that M-5 and M-25 are larger in diameter.

Another carbon nanofiller used to investigate the synergistic effect was 1-D carbon nanofiber (Pyrograf III CNF PR-19-XT-HHT) purchased from Pyrograf Products, Inc.

CNF has an average diameter of 150 nm which lies between that of carbon fiber and carbon nanotube. Unlike the perfect cylindrical structure wrapped from graphene of carbon nanotube, CNF is composed of numerous cup-shaped graphene layers stacked together. A comparison of the structures of CNF and CNT is shown in Figure 4-2.

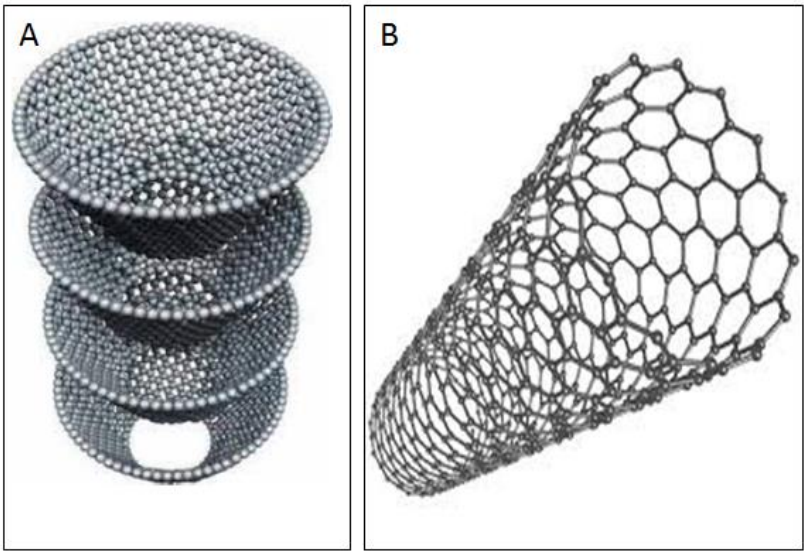

Figure 4-2 Comparison of CNF and CNT A: stacked-cup structure of CNF,

4.2.2 Matrix

The polymer matrix selected for this study was EPON^{TM} 862 (diglycidyl ether of bisphenol F), a low viscosity, colourless liquid epoxy resin. A non-methylene dianiline aromatic amine EPIKURE^{TM} W (diethyltoluenediamine) was used as the curing agent for this resin system. The electrical conductivity of neat epoxy was 6.5 x 10^{-9} S/cm, obtained from the product bulletin. The chemical structures of these chemicals as well as the crosslinking reaction are shown in Figure 4-3.

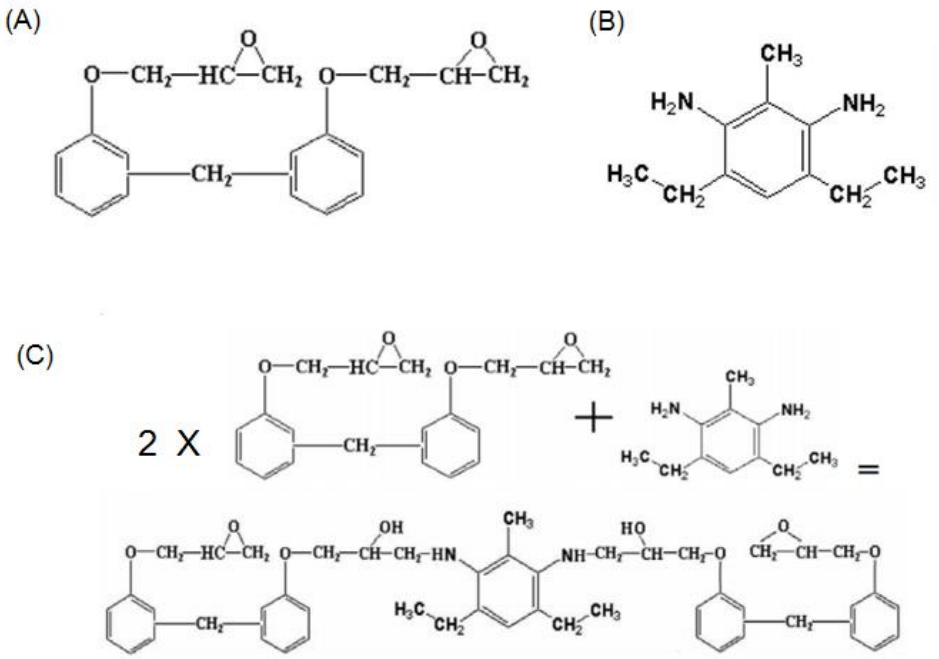

Figure 4-3 Chemical structure of epoxy and crosslinking reaction

4.2.3 Fabrication of Nanocomposites

A calculated amount of fillers were first dispersed in acetone a using 20 mL glass vial and were sonicated for one hour using an ultrasonication bath (Branson 5510). Epoxy resin was then added to the filler suspension and subjected to sonication for another hour. For the regular method, acetone was evaporated by heating and magnetic stirring on a hot plate for 5 hours. For the hot sonication method, the mixture was kept in the same ultrasonication bath with the heating function on. The volatile acetone could be gradually evaporated by sonication at 50°C for a similar period as the regular method. Next, the epoxy/filler mixture was allowed to cool down to room temperature to prevent premature curing. The stoichiometric amount of curing agent based on the epoxy to curing agent

ratio of 100:26 by weight was then added under continuous stirring. To avoid bubbles, the mixture was degassed in a vacuum chamber for 30 min, before the curing step. Finally, the mixture was spread onto a glass slide wrapped with aluminum foil using an adjustable film applicator and was cured at 100°C for 2 hours, followed by post-curing at 150°C for 2 hours. The schematic for the fabrication of nanocomposites is shown in figure 4-4.

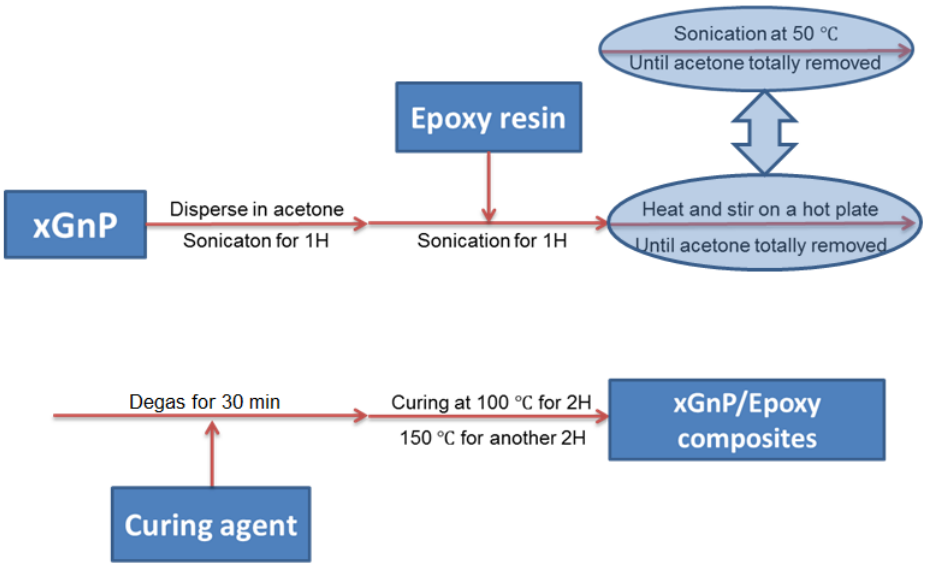

Figure 4-4 Schematic of fabrication of nanocomposites

4.2.4 Conductivity Measurement

The electrical conductivities of fillers and of composites were determined by four-probe methods. All composite samples were carefully polished and were then cut into small pieces to fit the custom 4-probe stage. A multi-channel electrochemical testing platform (VersaSTAT MC, Princeton Applied Research, USA) was used to supply steady

current through the outer 2 probes and measure the voltage between the inner 2 probes. The four probes were equally spaced at 0.15 cm. Based on the average current (*I*,A) and voltage (*V*, V) readings and the dimensions of the samples, the electrical conductivities (σ , S/cm) were calculated using the following equation.

$$\sigma = \frac{1}{\rho} = \frac{l}{RA} = \frac{Il}{VTW}$$

Where *l* is the spacing between each probe (cm), *T* is the thickness (cm) and *W* is the width of sample (cm).

4.3 Results and Discussions

4.3.1 Comparison of Liquid Phase Exfoliated Graphene and xGnP

As introduced in Chapter 3, few-layer graphene was successfully produced by the direct exfoliation of three different kinds of graphite in gum Arabic aqueous solutions. Thus-obtained pristine graphene exhibited desirable properties including low defect and high electrical conductivity. Also, the production scales were large enough to provide a sufficient quantity of fillers for the fabrication of composites. However, mixing liquid-phase exfoliated graphene (LEG) with polymers has not yet been well studied. Only a handful of studies that use LEGs as mechanical reinforcement fillers in polyurethane [8], polyvinylalcohol [9] and polylactide [10]have been done. In these studies, polymers were directly added to the graphene dispersions because the exfoliation medium were all mutual solvents for graphene and polymer matrices.

On the other hand, xGnPs are short stacks of several layers of graphene sheets produced by thermal expansion or microwave exfoliation of graphite intercalated compound (GIC) [11]. Following a size reduction process, xGnPs with a thickness ranging from 2 to 6 nanometers and diameter ranging from 1 to 25 microns are available. Figure 4-5 is an illustration of the xGnP structure. The compatibility of xGnP with most polymer matrices, as well as its unique platelet shape and pure graphitic composition, make it especially suitable for electrical conductivity enhancement. Additionally, the cost of xGnP is significantly lower than commonly used nanotubes.

LEGs and xGnPs are all synthesized by non-oxidizing processes, and the pristine graphitic structures are preserved. Representative SEM images of LEG (A) and xGnP (B) are compared in Figure 4-6. It is clear that the morphologies of these two kinds of graphene are similar. The difference, in terms of lateral dimensions, is that LEG exhibits a smaller size (mostly less than 1 μm) as well as higher polydispersity, while each grade of xGnP has a narrow distribution and a larger average diameter (up to 25 μm). The polydispersity of lateral dimension has been recognized as an inevitable shortcoming of the liquid phase exfoliation process, due to the sonication-induced cleavage effect [12], and the performance of thus-obtained graphene decreases as a consequence. Moreover, the electrical conductivities of xGnPs (648.6-739.6 S/cm) are more than 2 times higher than those of LEGs (235.2-280.9 S/cm), which is evidently more favorable for the improvement of the electrical properties of nanocomposites. So far, LEGs produced by the current procedure have not outperformed the commercial xGnPs as fillers for electrical property enhancement of polymer nanocomposites.

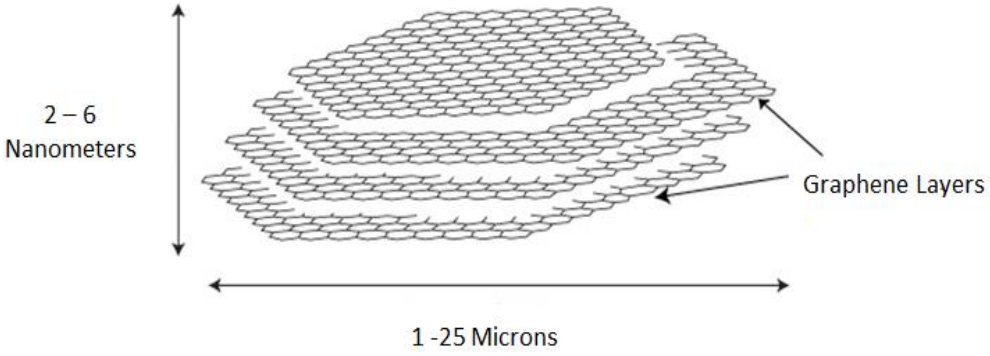

Figure 4-5 Illustration of xGnP structure

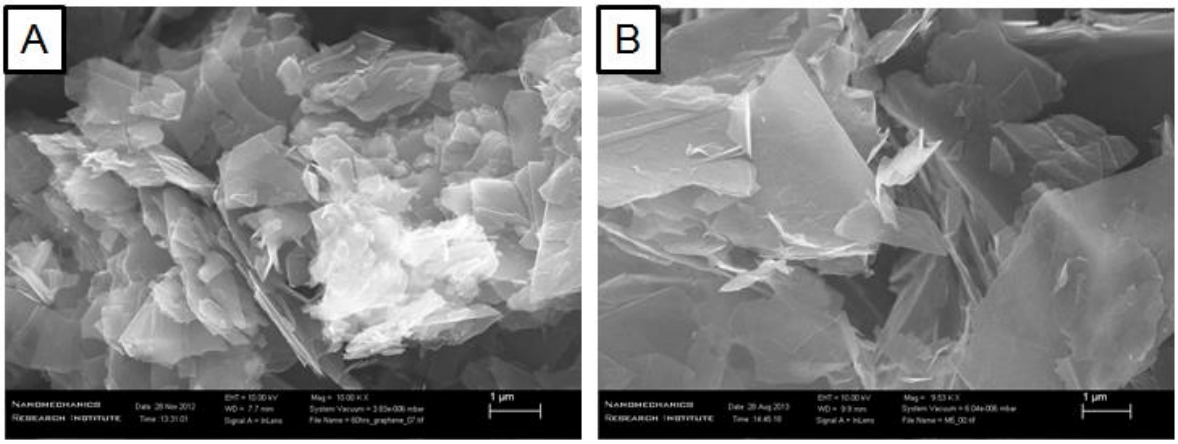

Figure 4-6 Comparison of LEG and xGnP

4.3.2 Effect of the Aspect Ratio of Filler

The aspect ratio of conducting filler, defined as the ratio of its longest dimension to

its shortest one, has been considered as one of the most important factors in making electrical conductive composites. For filler with a flake-like shape such as graphene platelet, the aspect ratio is simply the ratio of the lateral diameter to flake thickness. Four different grades of xGnPs, with different aspect ratios (500 for C-750, 833 for M-5, 1000 for C-300 and 4176 for M-25), were dispersed into epoxy matrices at 5 wt.% and 10 wt.%. The results of composite conductivities are presented in Figure 4-7. At 5 wt.% loadings, only the composites filled with M-25, which has the largest aspect ratio showed one order of conductivity improvement from neat epoxy. When the loadings were doubled, the conductivity of M-25/epoxy became 5 orders of magnitude higher than that of neat epoxy. Composite filled with C-300, the one with the second largest aspect ratio, also displayed one order of conductivity increase at 10 wt.%. However, enhancements of conductivities for C-750 and M-5 still haven't been observed at 10 wt.%. Conductive paths might be formed for composites filled with C-750 and M-5 by further increasing the loadings, but it will result in processing difficulties and poorer mechanical properties.

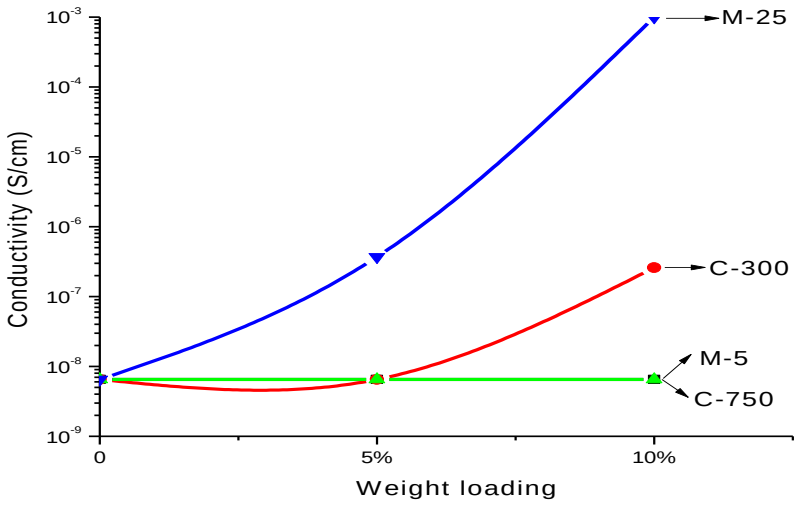

Figure 4-7 Results of composite conductivities

It is widely recognized that a conductive path is easier to form by dispersing fillers with higher aspect ratios into the polymer matrix [11,13]. In this study, M-25 has a much higher aspect ratio than the other three types of xGnPs. As expected, M-25 was the only one that formed a conductive path in the epoxy matrix at 5 wt.%. The conductivity of composites filled with 10 wt.% M-25 was much higher than those filled with the other three xGnPs, which could be explained as the lower contact resistance of a conductive path formed by larger sheets. As seen in the SEM images in Figure 4-8, conductive networks are formed in epoxy matrices both by 10 wt.% C-300 and 10 wt.% M-25. However, there are fewer sheet-sheet junctions along each conductive path created by M-25, due to its larger size, thus resulting in higher bulk conductivity.

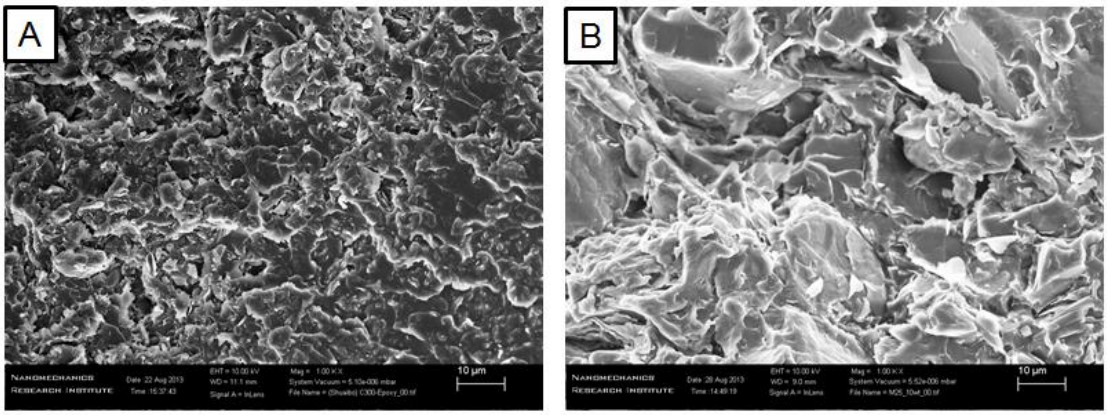

Figure 4-8 Comparison of composite morphologies filled with C-300 (A) and M-25 (B)

4.3.3 Effect of the Dispersion State and Hot Sonication

Other than the filler's intrinsic properties, such as aspect ratio, the dispersion state of fillers also strongly affects the properties of nanocomposites, and the degree of dispersion mainly depends on the method used for composite fabrication. To obtain better dispersion and properties, various techniques have been developed including covalent functionalization [14], surfactant stabilization [15,16] and polymer stabilization[17]. All of the above techniques can effectively improve the dispersions, however, covalent bonding disrupts the pristine graphene structure and stabilizer somehow hampers the electrical property of composite.

With this in mind, in this study, a simple and non-destructive modification was made to the regular processing method of epoxy nanocomposites. After carefully evaluating the process, the regular solvent removal step was considered to have the highest chance of graphene re-aggregation due to its long duration and undisturbed condition. Therefore,

instead of heating and stirring on a hot plate, sonication in hot water was used for the evaporation of solvent. For 10 wt.% xGnP/epoxy composite applying hot sonication, the conductivity reached 0.025 S/cm from 0.001 S/cm for the regular method, already meeting the conductivity requirement for EMI shielding materials. SEM was used to visualize the dispersion state within epoxy matrix. As shown in Figure 4-9, compared with the regular method, the dispersion is more homogenized with no distinct aggregation for composite produced by hot sonication technique. The improvement in conductivity and the change in morphology all indicate that the hot sonication technique results in better dispersion and effectively prevents re-aggregating during the solvent removal step. This technique can be further used for other solution blending based processing, when the solvent is as volatile as acetone.

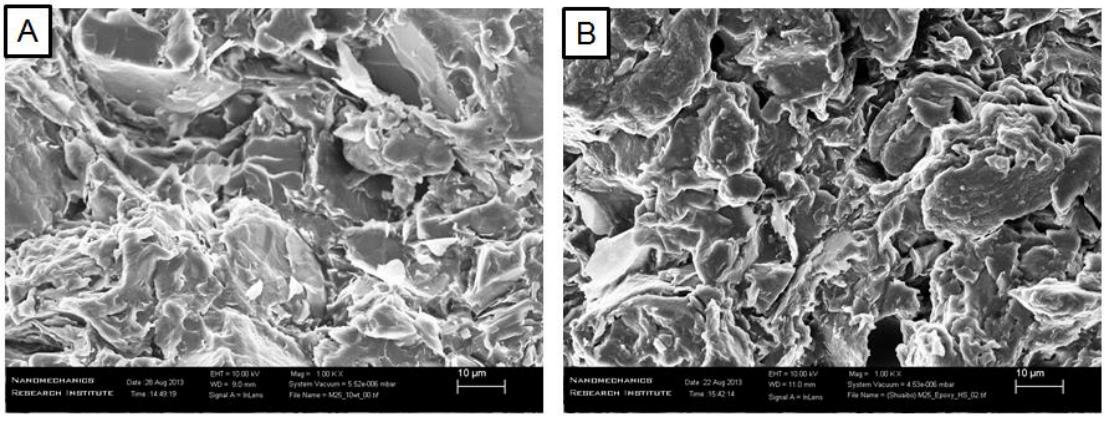

Figure 4-9 Comparison of regular method (A) and hot sonication method (B)

4.3.4 Effect of Adding Second Filler

The conductive path within the polymer matrix can be formed not only by dispersing one type of filler but also by combining two different types of fillers. Dispersing two types of fillers with different geometric shapes can obtain a synergy effect. For example, Ma et al. reported that adding a small fraction of one-dimensional carbon nanotube into zero-dimensional carbon black/epoxy composite optimized the poor connection between the carbon black, thus significantly enhancing the electrical conductivity [18]. Carbon nanotube has also been combined with two-dimensional xGnP to fabricate highly conductive nanocomposites for bipolar plates of fuel cells [19]. Carbon nanofiber (CNF) is another highly conductive rod-like filler, which is much cheaper than carbon nanotube. In this study, 1 wt.% of CNF and 4 wt.% xGnP-M25 were simultaneously dispersed in the epoxy matrix by the regular process. The resultant conductivity of the composite with hybrid filler was 5.18×10^{-3} S/cm. Compared to the conductivity of composite comprising solely xGnP, this was 4 orders of magnitude higher. As shown in Figure 4-10, the long flexible CNFs connect the planer xGnPs, forming a more effective conductive network. The sheet-sheet contact resistance is remarkably reduced by adding highly conductive CNF.

Unfortunately, the hot sonication technique is not applicable for the hybrid system, since the unique stacked-cup structure of CNF is vulnerable to long-term sonication. No better result was obtained by the attempt of applying hot sonication to the hybrid system, and the evidence of the shortened fibers is presented in Figure 4-11.

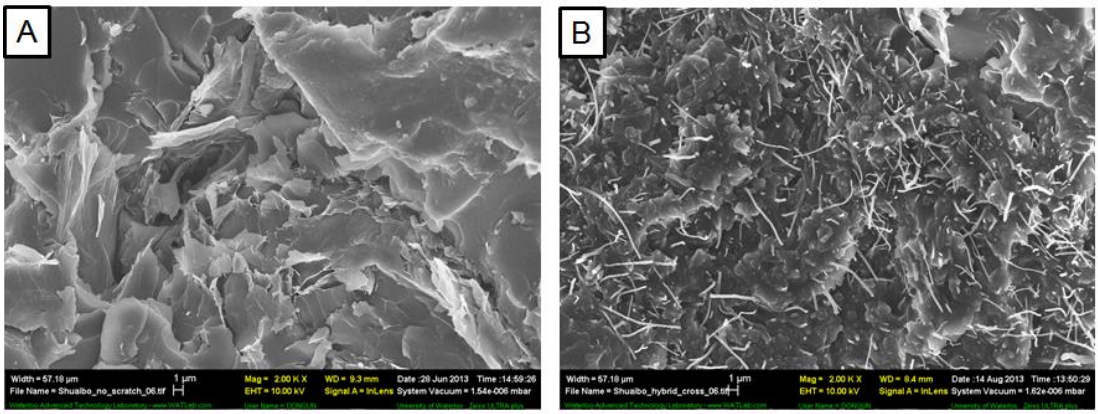

Figure 4-10 Comparison of pure xGnP (A) and hybrid filler system (B)

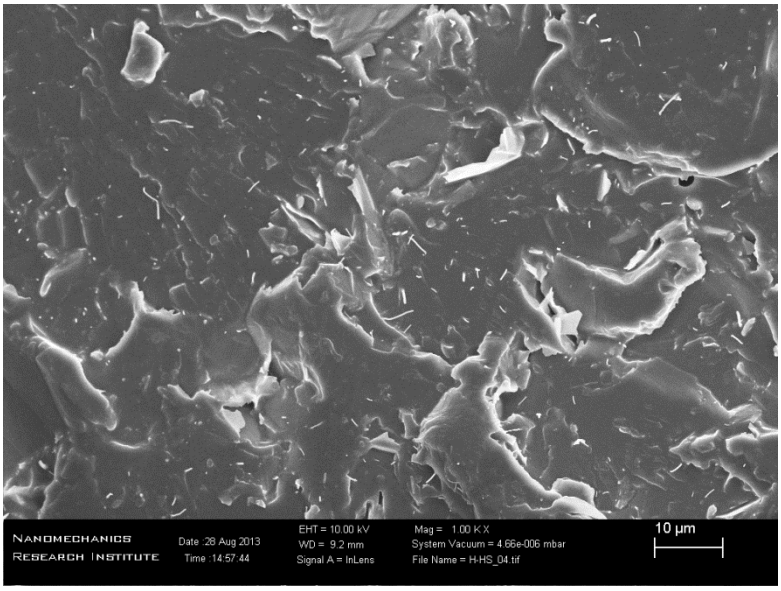

Figure 4-11 Hot sonication on hybrid filler system

4.5 Conclusions

In this work, commercial xGnPs were first compared with the self-produced LEGs in terms of morphology, conductivity, and aspect ratios. It was found that the polydispersity of the lateral size for LEG was not favorable for electrical conductivity enhancement. Then, four different grades of xGnPs were dispersed into an epoxy matrix to make electrical conductive nanocomposites. M-25, the one with the largest mean lateral size and aspect ratio, showed the best performance. The conductivity of composites filled with 10 wt.% M-25 was five orders of magnitude higher than that of neat epoxy. A better dispersion state and less aggregation have been achieved by using hot sonication instead of the regular heating and stirring method to remove solvent. The highest conductivity obtained was 0.025 S/cm based on 10 wt.% M-25 and hot sonication, which meets the conductivity requirement for EMI shielding materials. The simple and effective hot sonication technique offers a new solution for preventing graphene re-aggregation during the solvent removal step. Additionally, xGnP was combined with stacked-cup CNF for the first time, and the composite conductivity was significantly improved due to the synergic effect.

References

[1] L. Vescovo, M. Sangermano, R. Scarazzini, G. Kortaberria, I. Mondragon, In-situ-Synthetized Silver/Epoxy Nanocomposites: Electrical Characterization by Means of Dielectric Spectroscopy, Macromol. Chem. Phys. 211 (2010) 1933-1939.

[2] F. Tan, X. Qiao, J. Chen, H. Wang, Effects of coupling agents on the properties of epoxy-based electrically conductive adhesives, Int J Adhes Adhes. 26 (2006) 406-413.

[3] R.M. Mutiso, K.I. Winey, 7.17 - Electrical Conductivity of Polymer Nanocomposites, in: K. Matyjaszewski, M. Möller (Eds.), Polymer Science: A Comprehensive Reference, Elsevier, Amsterdam, 2012, pp. 327-344.

[4] M. Wen, X. Sun, L. Su, J. Shen, J. Li, S. Guo, The electrical conductivity of carbon nanotube/carbon black/polypropylene composites prepared through multistage stretching extrusion, Polymer. 53 (2012) 1602-1610.

[5] S. Kim, L.T. Drzal, Comparison of Exfoliated Graphite Nanoplatelets (xGnP) and CNTs for Reinforcement of EVA Nanocomposites Fabricated by Solution Compounding Method and Three Screw Rotating Systems, J. Adhes. Sci. Technol. 23 (2009) 1623-1638.

[6] R. strümpler, J. Glatz-Reichenbach, Conducting Polymer Composites, Journal of Electroceramics. 3 (1999) 329-346.

[7] J. Huang, EMI shielding plastics: A review, Adv. Polym. Technol. 14 (1995) 137-150.

[8] U. Khan, P. May, A. O'Neill, J.N. Coleman, Development of stiff, strong, yet tough composites by the addition of solvent exfoliated graphene to polyurethane, Carbon. 48 (2010) 4035-4041.

[9] P. May, U. Khan, A. O'Neill, J.N. Coleman, Approaching the theoretical limit for reinforcing polymers with graphene, Journal of Materials Chemistry. 22 (2012) 1278-1282.

[10] X. Li, Y. Xiao, A. Bergeret, M. Longerey, J. Che, Preparation of polylactide/graphene composites from liquid‐phase exfoliated graphite sheets, Polymer Composites. 35 (2014) 396-403.

[11] H. Fukushima, Graphite nanoreinforcements in polymer nanocomposites, ProQuest Dissertations and Theses. (2003).

[12] W. Du, X. Jiang, L. Zhu, W. Du, X. Jiang, L. Zhu, From graphite to graphene: direct liquid-phase exfoliation of graphite to produce single- and few-layered pristine graphene, Journal of Materials Chemistry A. 1 (2013) 10592-10606.

[13] H.-. Park, K. Kalaitzidou, H. Fukushima, L.T. Drzal, Exfoliated graphite nanoplatelet (xGnP)/polypropylene nanocomposites, SPE Automotive and Composites Divisions - 7th Annual Automotive Composites Conference and Exhibition, ACCE 2007 - Driving Performance and Productivity. 1 (2007) 314-322.

[14] S.G. Miller, J.L. Bauer, M.J. Maryanski, P.J. Heimann, J.P. Barlow, J. Gosau, R.E. Allred, Characterization of epoxy functionalized graphite nanoparticles and the physical properties of epoxy matrix nanocomposites, Composites Sci. Technol. 70 (2010) 1120-1125.

[15] S. Stankovich, D.A. Dikin, G.H.B. Dommett, K.M. Kohlhaas, E.J. Zimney, E.A. Stach, R.D. Piner, S.T. Nguyen, R.S. Ruoff, Graphene-based composite materials, Nature. 442 (2006) 282-286.

[16] S. Vadukumpully, J. Paul, N. Mahanta, S. Valiyaveettil, Flexible conductive graphene/poly(vinyl chloride) composite thin films with high mechanical strength and thermal stability, Carbon. 49 (2011) 198-205.

[17] A.S. Wajid, H.S.T. Ahmed, S. Das, F. Irin, A.F. Jankowski, M.J. Green, High-Performance Pristine Graphene/Epoxy Composites With Enhanced Mechanical and Electrical Properties, Macromolecular Materials and Engineering. 298 (2013) 339-347.

[18] P.-.C. Ma, M.-.Y. Liu, H. Zhang, S.-.Q. Wang, R. Wang, K. Wang, Y.-.K. Wong, B.-.Z. Tang, S.-.H. Hong, K.-.W. Paik, J.-.K. Kim, Enhanced electrical conductivity of nanocomposites containing hybrid fillers of carbon nanotubes and carbon black, 1 (2009) 1090-1096.

[19] M. Kim, Gu-hyeok Kang, W.P. Hyung, Young-bin Park, Y.H. Park, H.Y. Kwan, Design, Manufacturing, and Characterization of High- Performance Lightweight Bipolar Plates Based on Carbon Nanotube- Exfoliated Graphite Nanoplatelet Hybrid Nanocomposites, Journal of Nanomaterials. 2012 (2012).

CHAPTER 5： Conclusions and Recommendations

5.1 Conclusions

In this study, few-layer graphene has been successfully produced by liquid phase exfoliation in a gum Arabic aqueous solution. Three types of graphite of different sizes were studied as starting materials. Low defect ratios and relatively high conductivities were observed for all graphene products. With the exception of the graphite with the largest size, the other two yielded considerable quantities of graphene in each batch. However, compared with the commercial xGnPs, LEGs showed polydispersity in terms of lateral size, which has been recognized as unfavorable for the electrical conductivity enhancement of nanocomposites.

M-25, with the largest aspect ratio, showed the best performance among the four types of xGnP. Five orders of magnitude of conductivity enhancements were obtained at 10 wt.% for the M-25/epoxy composite. The electrical conductivities of composites have been further improved either by applying a hot sonication technique or by adding a small amount of CNF. The highest conductivity obtained, 0.025 S/cm, has met the requirement for EMI shielding materials. Hot sonication technique has great potential to be used for other solution-based processes, and the combination of xGnP and CNF has created a new effective hybrid filler system that can be used to make electrical conductive polymer nanocomposites.

5.2 Recommendations

Based on the present results and a survey of literatures, several recommendations can be proposed for future works. First of all, a size selection step can be added at the end of the liquid phase exfoliation process to solve the problem of polydispersity. Specifically, a controlled centrifugation procedure is suggested to separate LEGs by lateral size. With a larger size and a narrower distribution, LEG might match the performance of xGnP in terms of conductivity enhancement for nanocomposites. Secondly, for the measurement of conductivity, it is better to use a standard four-probe method rather than the custom one, in order to obtain more accurate and constant results. Thirdly, more experiments about the hybrid system should be conducted, and the ratio of xGnP to CNF should be optimized.